Wind turbine wake characterization with optical remote sensing and computational fluid dynamics

MATTHEW L. AITKEN

ORISE Research Fellow, Environmental Protection Agency

(Former affiliation: Dept. of Physics, University of Colorado)

October 21, 2014

Acknowledgments

- Advisor: Julie Lundquist (CU/NREL)
- Dissertation committee
  - Michael Ritzwoller (CU)
  - Robert Banta (NOAA)
  - Judah Levine (CU/NIST)
  - Dmitri Uzdensky (CU)
- Other collaborators
  - Branko Kosović (NCAR)
  - Jeff Mirocha (LLNL)
  - Yelena Pichugina (NOAA)
  - Andy Clifton (NREL)

Outline

- Lidar background
- Wind turbine wake characterization
  - theory and previous work
  - wake detection algorithm
  - experiment
  - simulation
- Summary

Outline

- **Lidar background**
- Wind turbine wake characterization
  - theory and previous work
  - wake detection algorithm
  - experiment
  - simulation
- Summary

Pulsed coherent lidar principle of operation

- Transmitted optical signal is scattered from atmospheric aerosols advected by wind
- Return signal optically mixed w/ local oscillator
- Resulting beat frequency indicates Doppler shift due to moving particles
  - wind speed is proportional to Doppler shift
  - offset frequency added to local oscillator to distinguish between (+) and (-) velocities
- Only line-of-sight velocity can be discerned

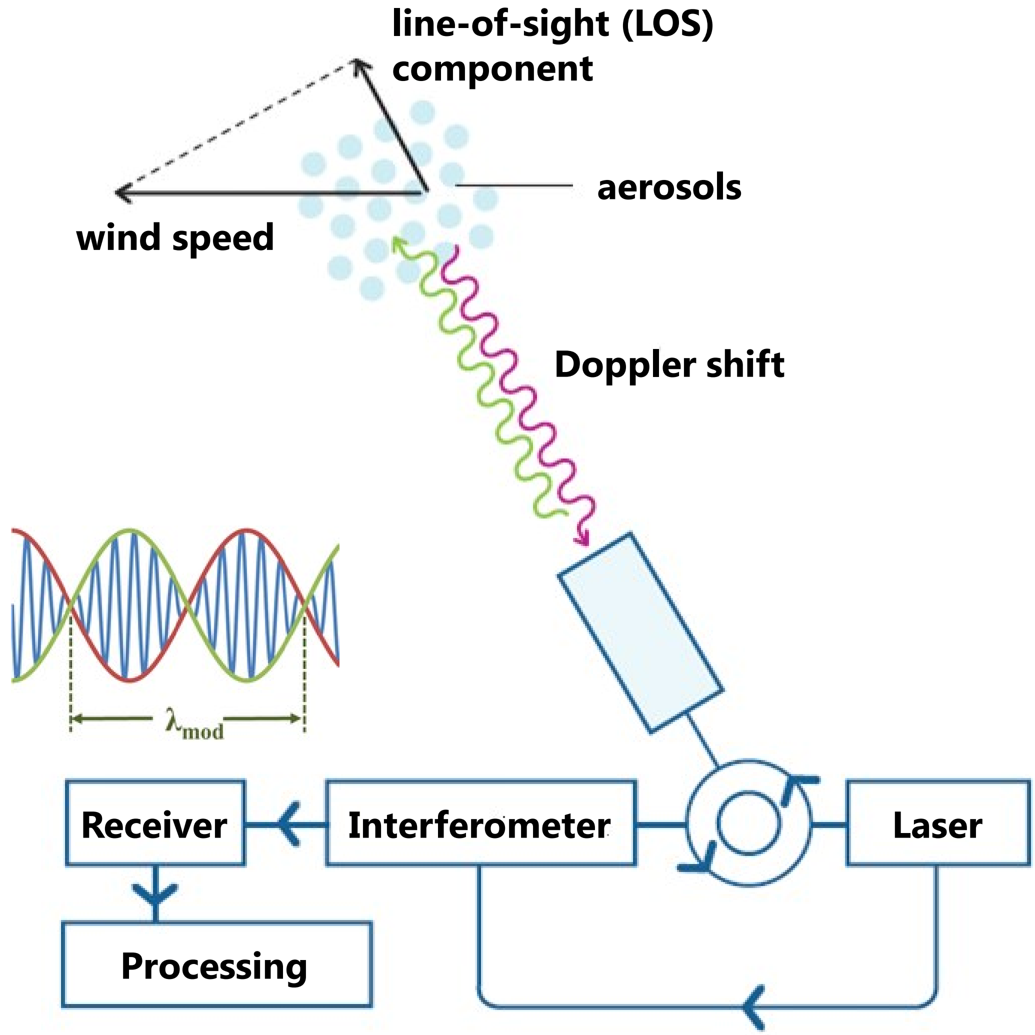

Fig: Leosphere

Lidar measurements taken usually under the assumption that the flow is homogeneous

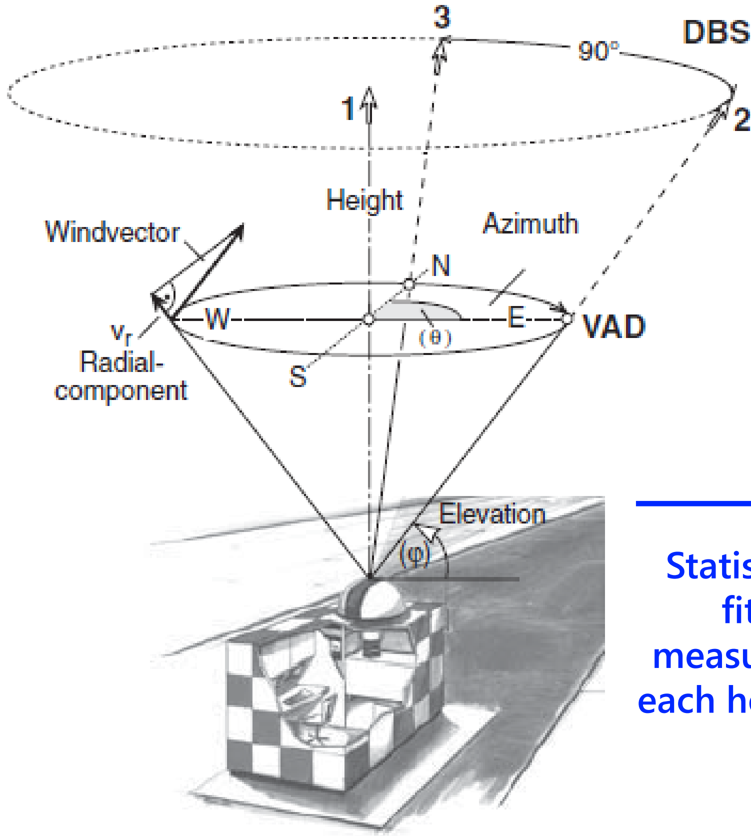

Statistical model fit to lidar measurements for each height interval

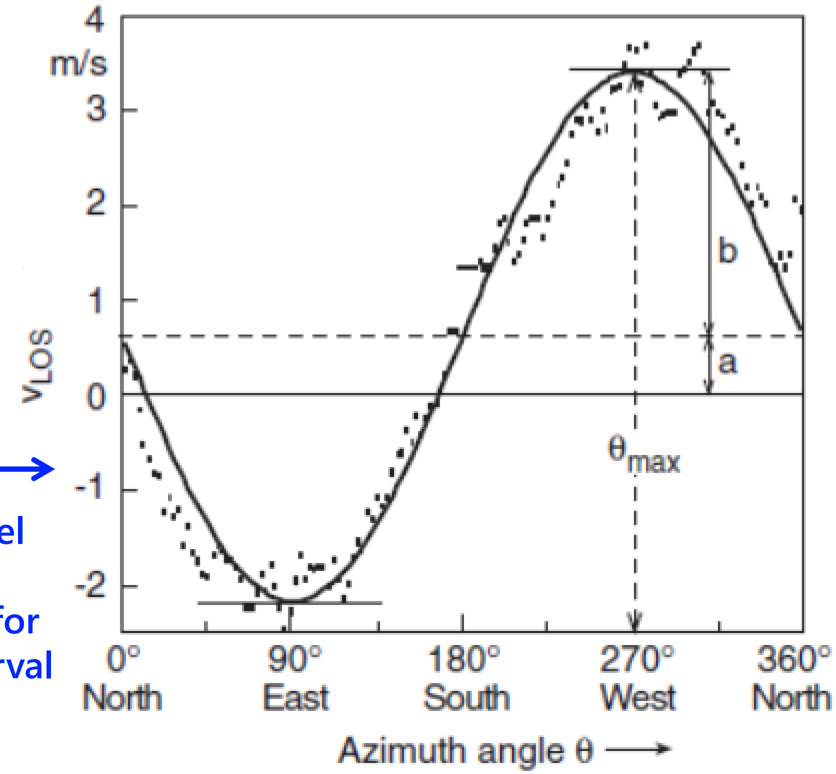

$$v_{\mathrm{LOS}} = -u \sin\theta \cos\phi - v \cos\theta \cos\phi - w \sin\phi$$

$$v_{\mathrm{LOS}} = a + b\cos(\theta - \theta_{\mathrm{max}})$$

$$\mathbf{v} = (u, v, w) = (-b \sin\theta_{\mathrm{max}} / \cos\phi, -b\cos\theta_{\mathrm{max}} / \cos\phi, -a / \sin\phi)$$

Figs: Werner (2005)

Lidar applications to wind energy

- Data assimilation for improved forecasting
- Nacelle-based turbine control systems
  - increase energy output
  - decrease structural damage
- Resource assessment
  - reduce uncertainty in annual energy production (AEP)
  - lower borrowing costs
  - improve return on investment (ROI)
- **Wind turbine wake characterization**
  - **CFD model verification**

Fig: Alfred Wegener Institute

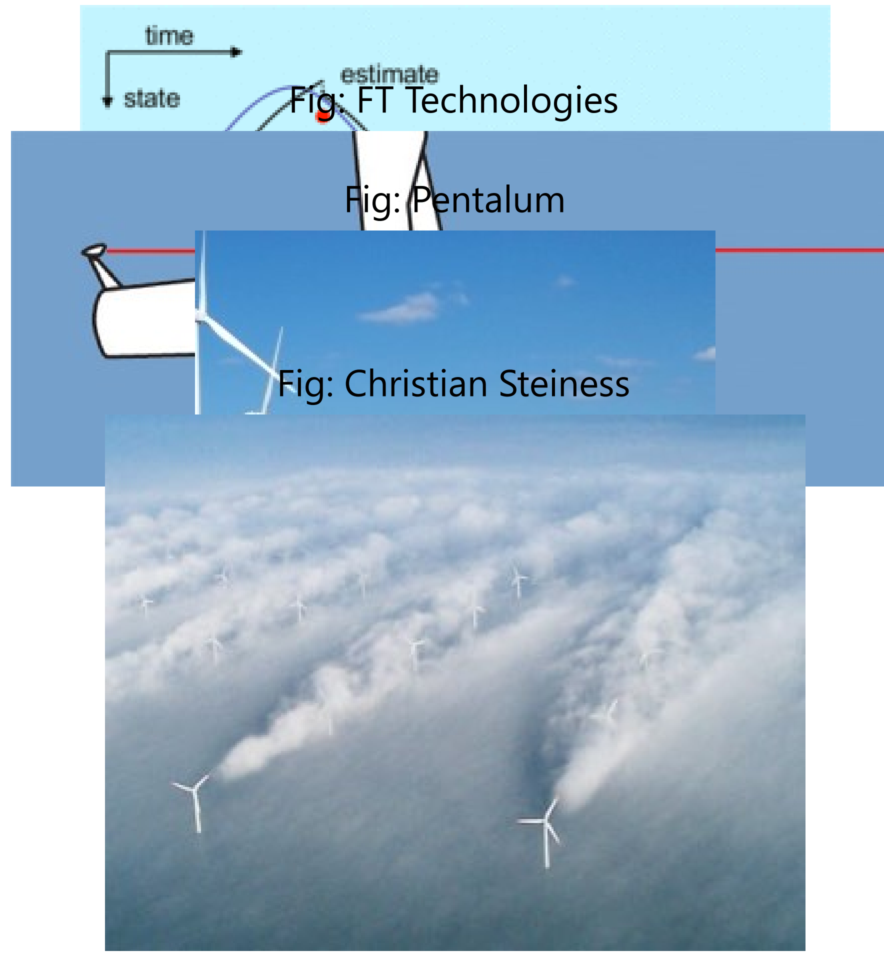

Fig: FT Technologies

Fig: Pentalum

Fig: Christian Steiness

Outline

- Lidar background
- **Wind turbine wake characterization**
  - **theory and previous work**
  - wake detection algorithm
  - experiment
  - simulation
- Summary

Wind turbine wakes are characterized by (1) velocity deficit & (2) increased turbulence…

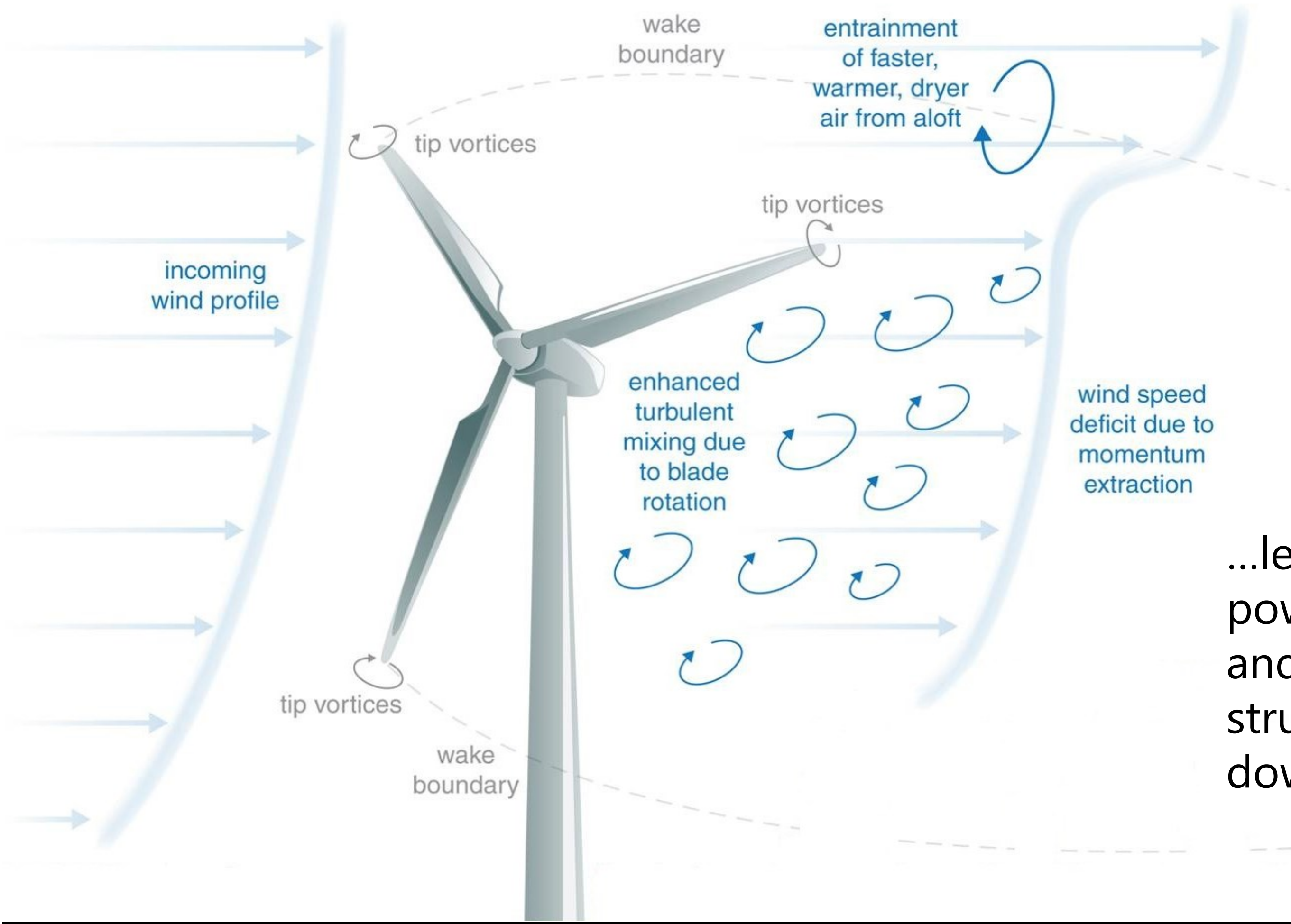

…leading to (1) lower power performance and (2) higher structural loading for downwind turbines

Fig: National Renewable Energy Laboratory

Motivation: to optimize turbine layouts and controls at wind farms

Sparse turbine layouts limit wake-induced **power losses** and **structural loading**...

...but dense layouts limit **costs** due to land, roads, and transmission.

Thus, there exists some intermediate spacing that optimizes **levelized cost**.

Power is maximized while capital, O&M, and transmission **costs** are minimized.

Wind turbine layout optimization

- Wind turbine wake modeling suffers from too much uncertainty
  - negatively impacts optimization of wind farm layouts
  - more experimental data needed for model verification
- Innovation in measurement techniques is increasingly important
  - scanning remote sensors offer fine resolution w/o disturbing flow
  - new methods are required to extract wake characteristics

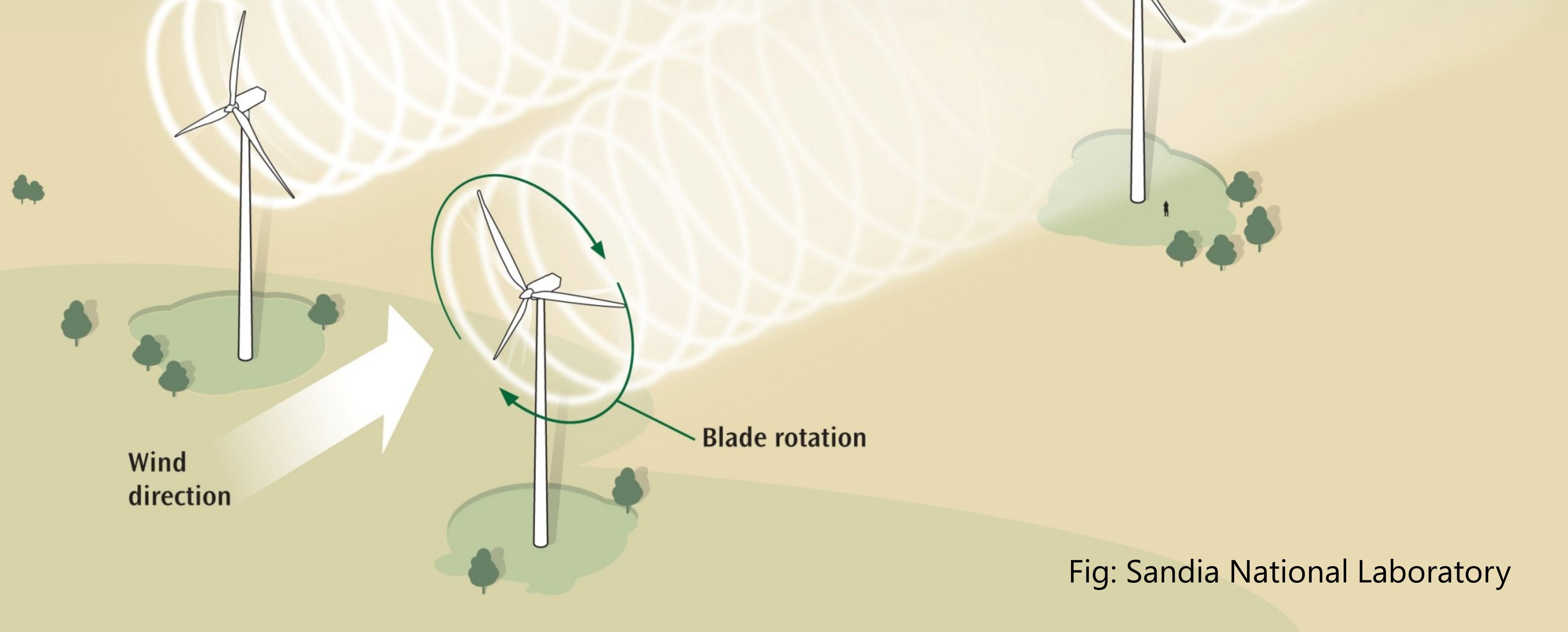

Fig: Sandia National Laboratory

Velocity deficit profile in the near and far wake

turbulent mixing causes the two local minima to merge into a single global minimum

amplitude decreases and width increases with distance behind the turbine

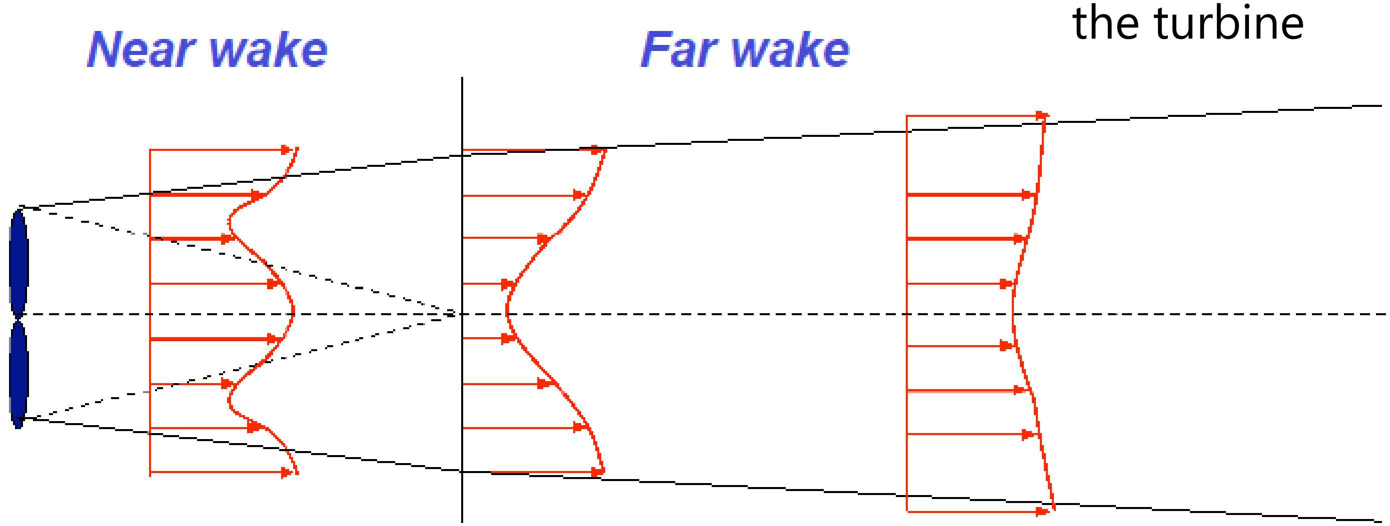

no rigid definition, but near wake usually taken to extend a few rotor diameters behind turbine

curve taken to be a Gaussian based on experimental evidence and similarity theory (Pope 2000)

Fig: Trujillo (2005)
IEA Annex XXIII workshop

Velocity deficit profile as simulated by WRF

- Just behind the turbine, the wake expands initially b/c of mass conservation
  - profile has two local minima
- In the far wake, the velocity deficit decreases and the wake boundary increases with downstream distance
  - turbulent mixing causes the ambient flow to be entrained within the wake
  - profile has one global minimum

Velocity deficit profile as simulated by WRF

- Just behind the turbine, the wake expands initially b/c of mass conservation
  - profile has two local minima
- In the far wake, the velocity deficit decreases and the wake boundary increases with downstream distance
  - turbulent mixing causes the ambient flow to be entrained within the wake
  - profile has one global minimum
- *x* = downstream distance
- D = rotor diameter

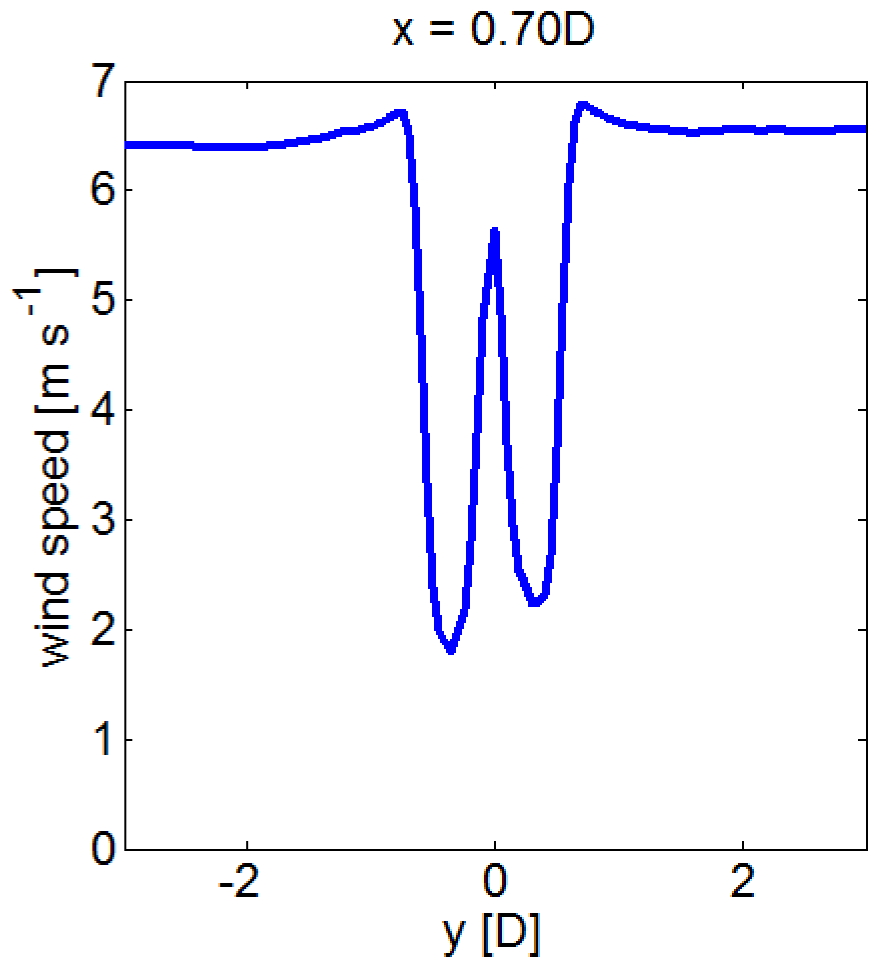

Previous wake measurements made using met towers, sodar, UAS, lidar, and radar

$$\text{VD} = \frac{u_{\text{ambient}} - u_{\text{wake}}}{u_{\text{ambient}}} \times 100\,\%$$

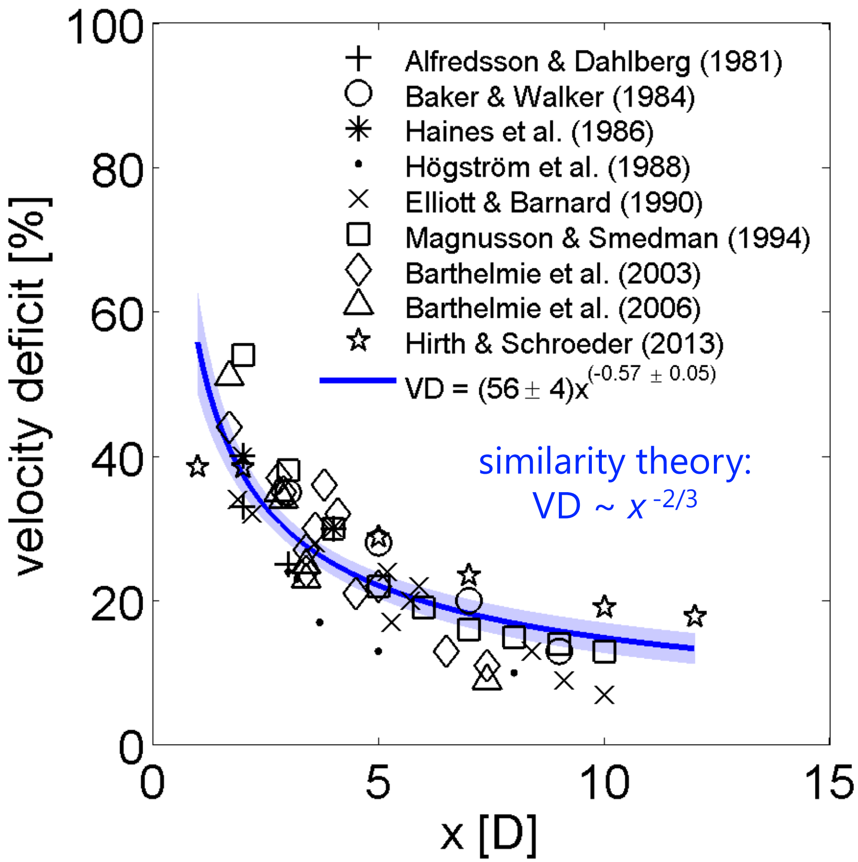

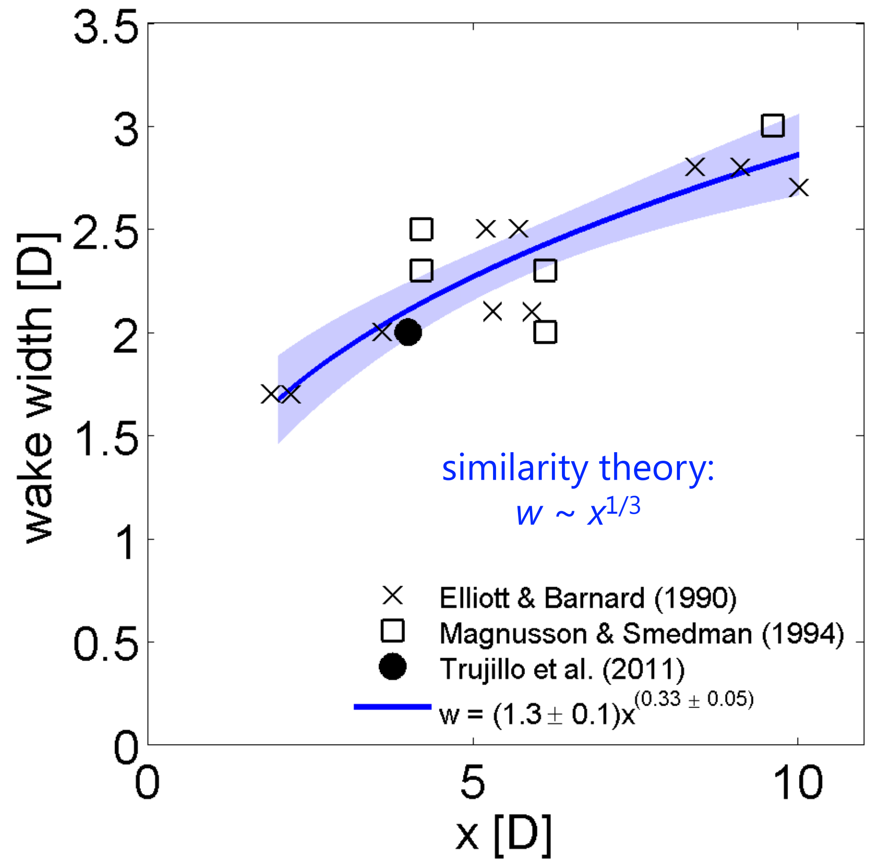

Aitken et al. (2014)
J. Atmos. Ocean. Tech., **31**, 765–787

Wake meandering driven by eddies with length scales on the order of the rotor

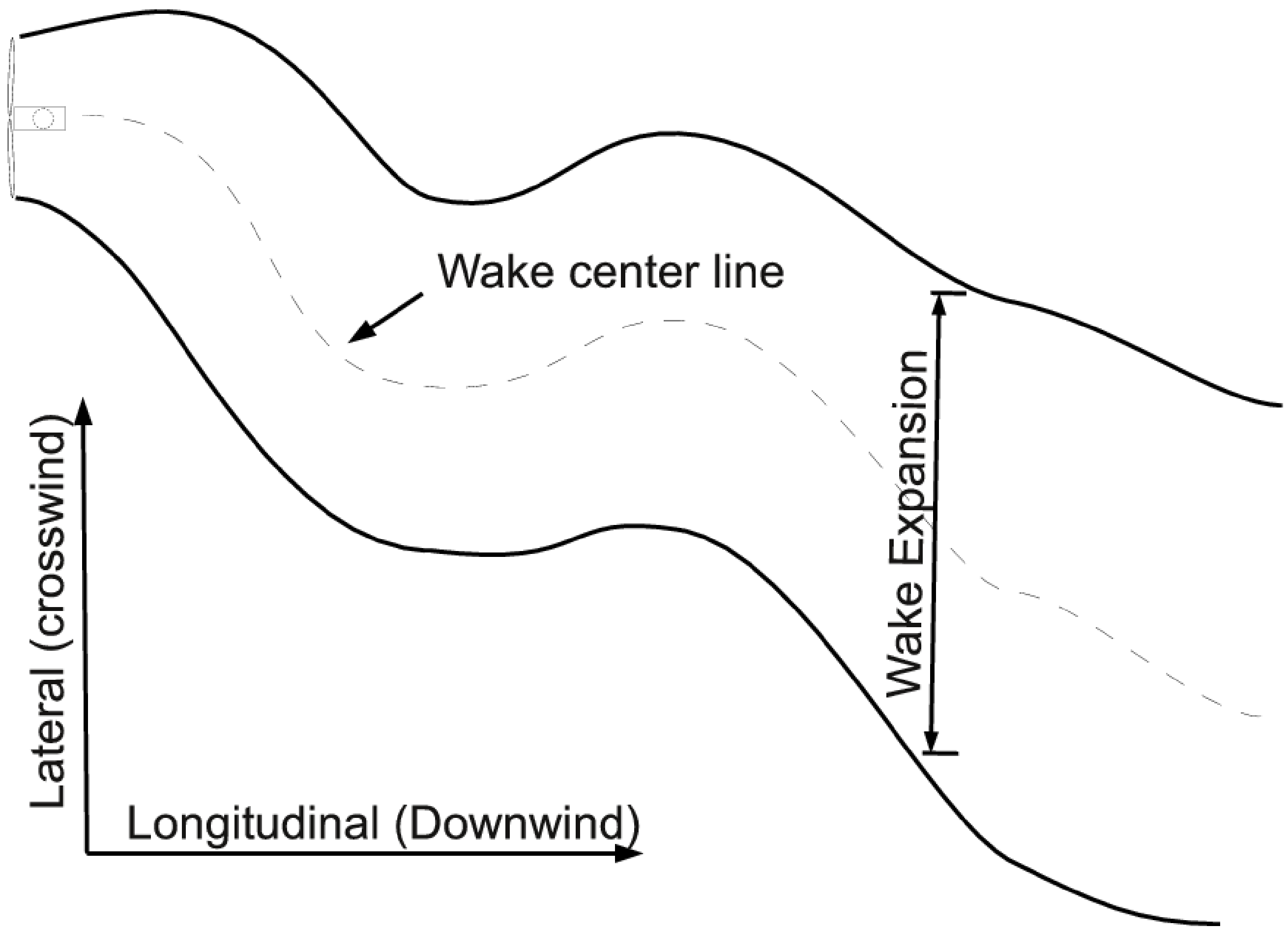

Fig: Larsen et al. (2008)
Wind Energy, **11**, 377–395

Uncertainty in the literature as to the vertical location of the wake centerline

- Wake center located *above* hub height
  - Magnusson and Smedman (1994); Helmis et al. (1995)
- Wake center located *at* hub height
  - Elliott and Barnard (1990); Kambezidis et al. (1990)
- Wake center located *near* hub height
  - Barthelmie et al. (2003)
- Wake center located *below* hub height
  - Crespo et al. (1988)

?

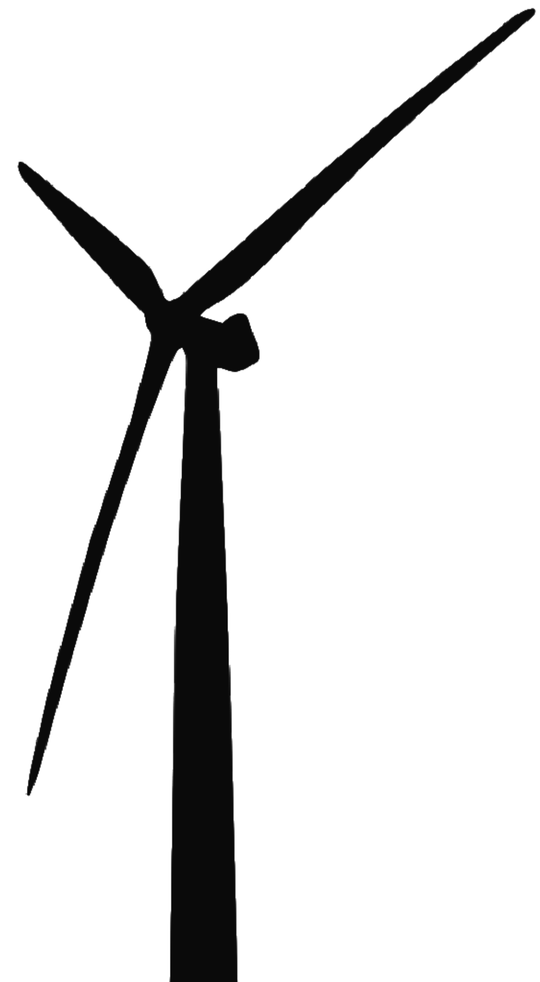

Improving upon wake characterization from previous remote sensing experiments

- Käsler et al. (2010): first long-range lidar study, but very brief analysis limited to a single scan
- Bingöl et al. (2010) and Trujillo et al. (2011)
  - nacelle-mounted ZephIR lidar with max range of 200 m
  - stall-regulated 95-kW test turbine w/ 29-m hub and 19-m rotor diameter
  - analysis focuses on horizontal wake meandering and is limited to just 10-min
- Hirth et al. (2012) and Hirth & Schroeder (2013): dual-Doppler radar methodology and wake tracking algorithm not readily generalized for application to other datasets
  - does not incorporate wake expansion
  - focuses mostly on tracking horizontal position of wake centerline
  - analysis limited to 1-hr period during rainfall
- Iungo et al. (2013): focuses mostly on testing various lidar scanning strategies
  - limited analysis of a few scans lasting 11 min each

Improving upon wake characterization from previous remote sensing experiments

- Need rigorous, general methodology for quantifying various wake characteristics
  - applicable to both remotely sensed measurements and numerical simulation output
- Need observations from modern pitch-regulated multi-MW turbines
- Need much more data to verify CFD models and to study effect of different atmospheric conditions
  - wind speed
  - turbulence
  - stability

Outline

- Lidar background
- Wind turbine wake characterization
  - theory and previous work
  - **wake detection algorithm**
  - experiment
  - simulation
- Summary

Lidar typically measures line-of-sight velocity (u_{LOS}) using two scanning strategies

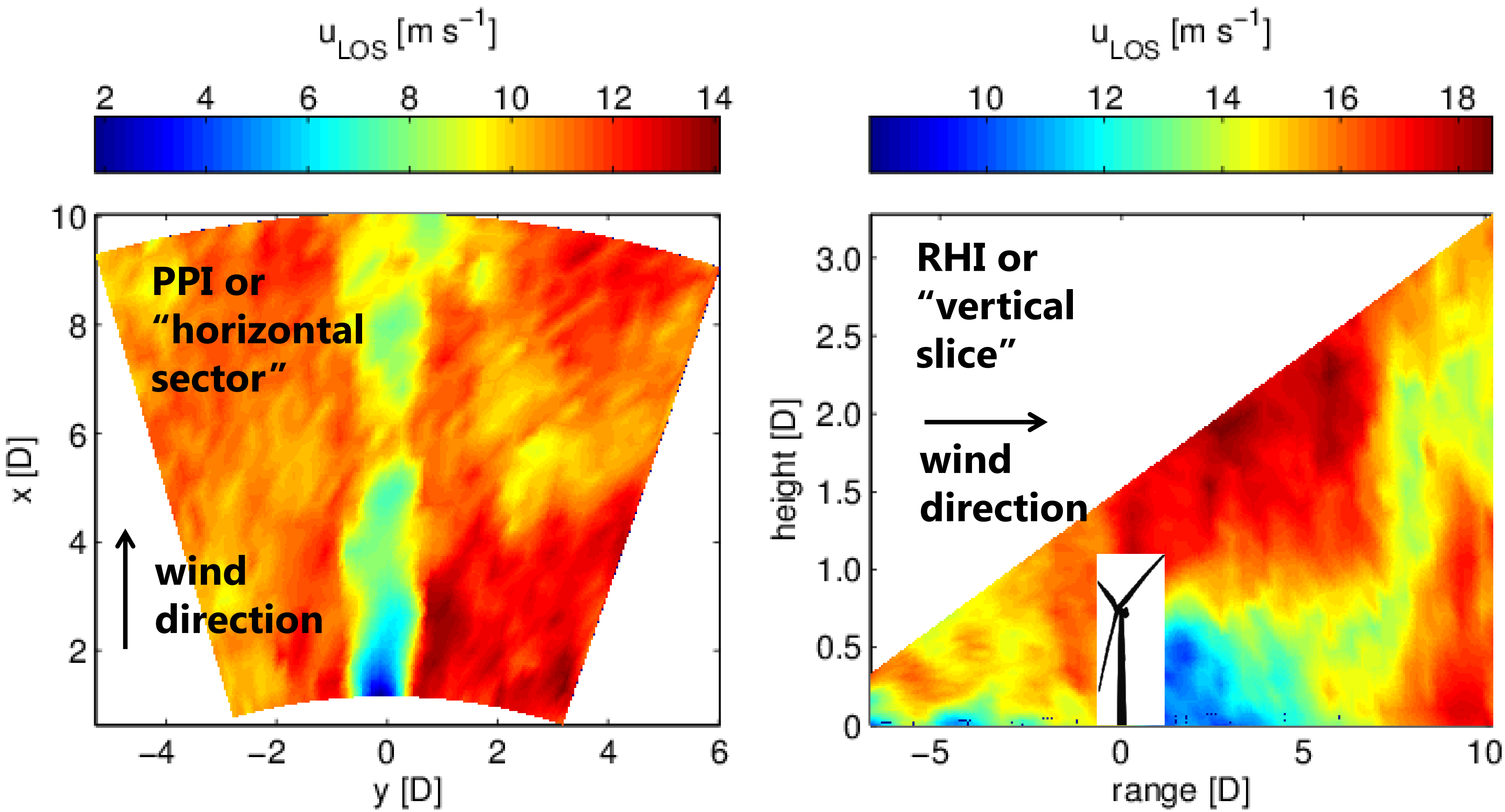

Aitken et al. (2014)
J. Atmos. Ocean. Tech., **31**, 765–787

Plan view of the coordinate systems with modeled parameters in purple

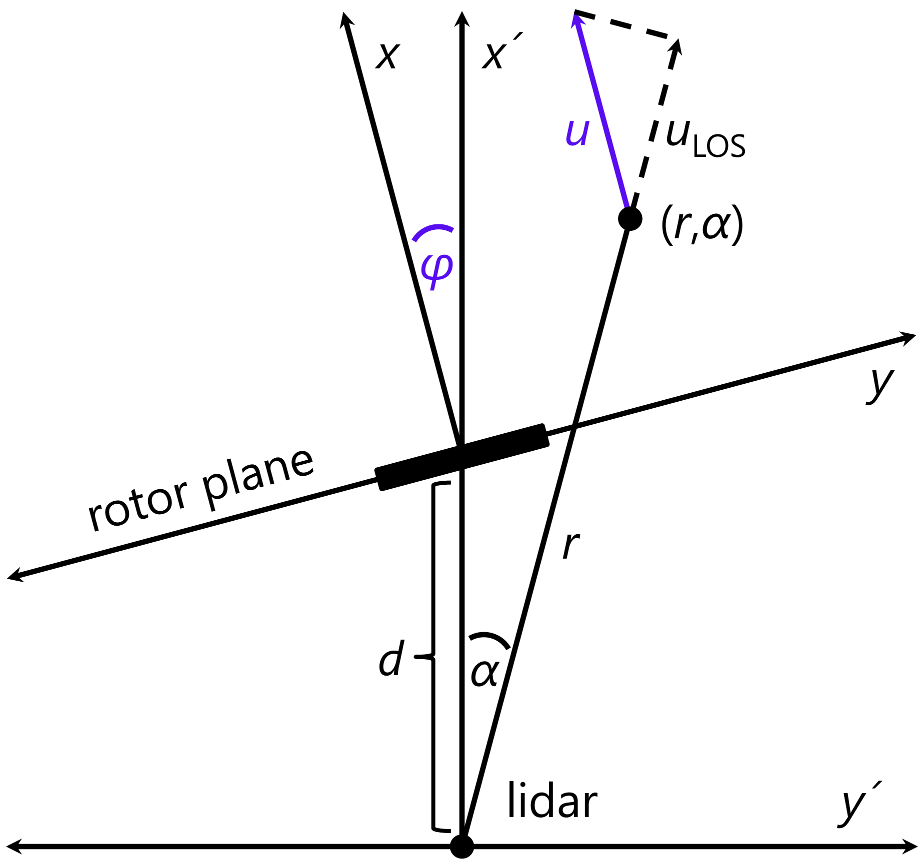

- d = distance from lidar to turbine
- r = lidar range gate
- α = lidar azimuth angle
- u = ambient wind speed
- φ = ambient wind direction
- u_{LOS} = line-of-sight velocity measured by lidar

Aitken et al. (2014)
J. Atmos. Ocean. Tech., **31**, 765–787

Wake modeled as Gaussian function subtracted from uniform ambient flow

For each beam sweep, and at each range gate *r*, three models are fit to the lidar data to identify the wake, if any → Extra sum-of-squares F-test used to find simplest model to fit data

$$u_{\mathrm{LOS}}(y',r) = u\cos(\alpha-\phi) = u\left(\frac{\sqrt{r^2-y'^2}}{r}\cos\phi + \frac{y'}{r}\sin\phi\right)$$

ambient flow model

$$u_{\mathrm{LOS}}(y',r) = \left(u - a\exp\left[\frac{-(y'-y_c)^2}{2s_w^2}\right]\right)\left(\frac{\sqrt{r^2-y'^2}}{r}\cos\phi + \frac{y'}{r}\sin\phi\right)$$

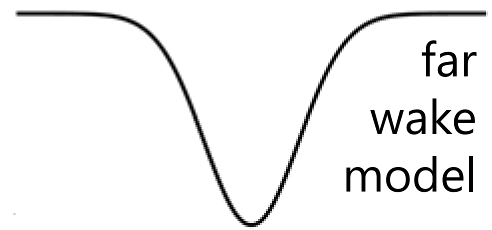

far wake model

$$u_{\mathrm{LOS}}(y',r) = \left(u - a\left\{\exp\left[\frac{-(y'-y_l)^2}{2s_w^2}\right] + \exp\left[\frac{-(y'-y_r)^2}{2s_w^2}\right]\right\}\right) \times \left(\frac{\sqrt{r^2-y'^2}}{r}\cos\phi + \frac{y'}{r}\sin\phi\right)$$

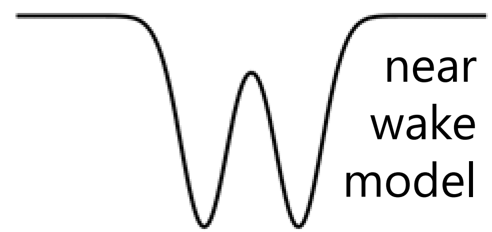

near wake model

Example fit to data from horizontal scan

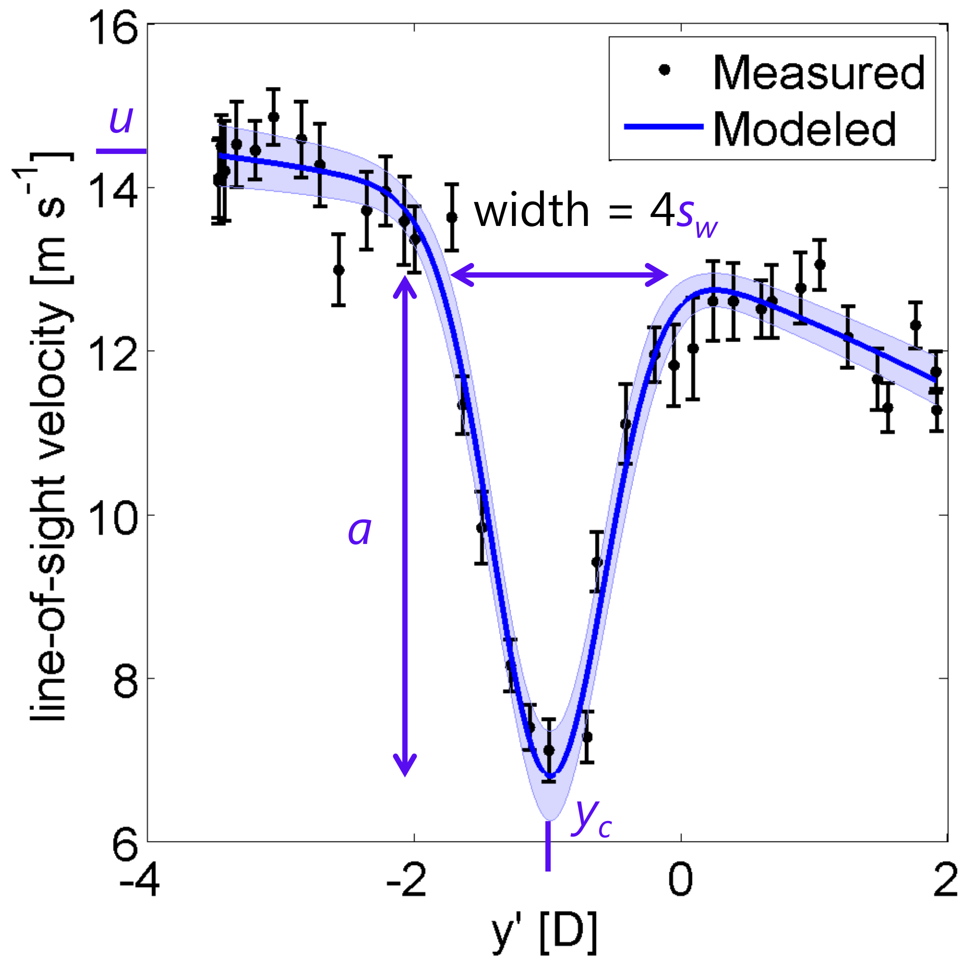

y_c: algorithm capable of tracking wake meandering

wake width ≡ $4s_w$
(Hansen et al. 2012)

$$\text{velocity deficit} \equiv \frac{u_{ambient} - u_{wake}}{u_{ambient}} \times 100\%$$

$$= \frac{u - (u - a)}{u} \times 100\%$$

$$= \frac{a}{u} \times 100\%$$

Aitken et al. (2014)
J. Atmos. Ocean. Tech., **31**, 765–787

Side view of the coordinate systems used for vertical scan model

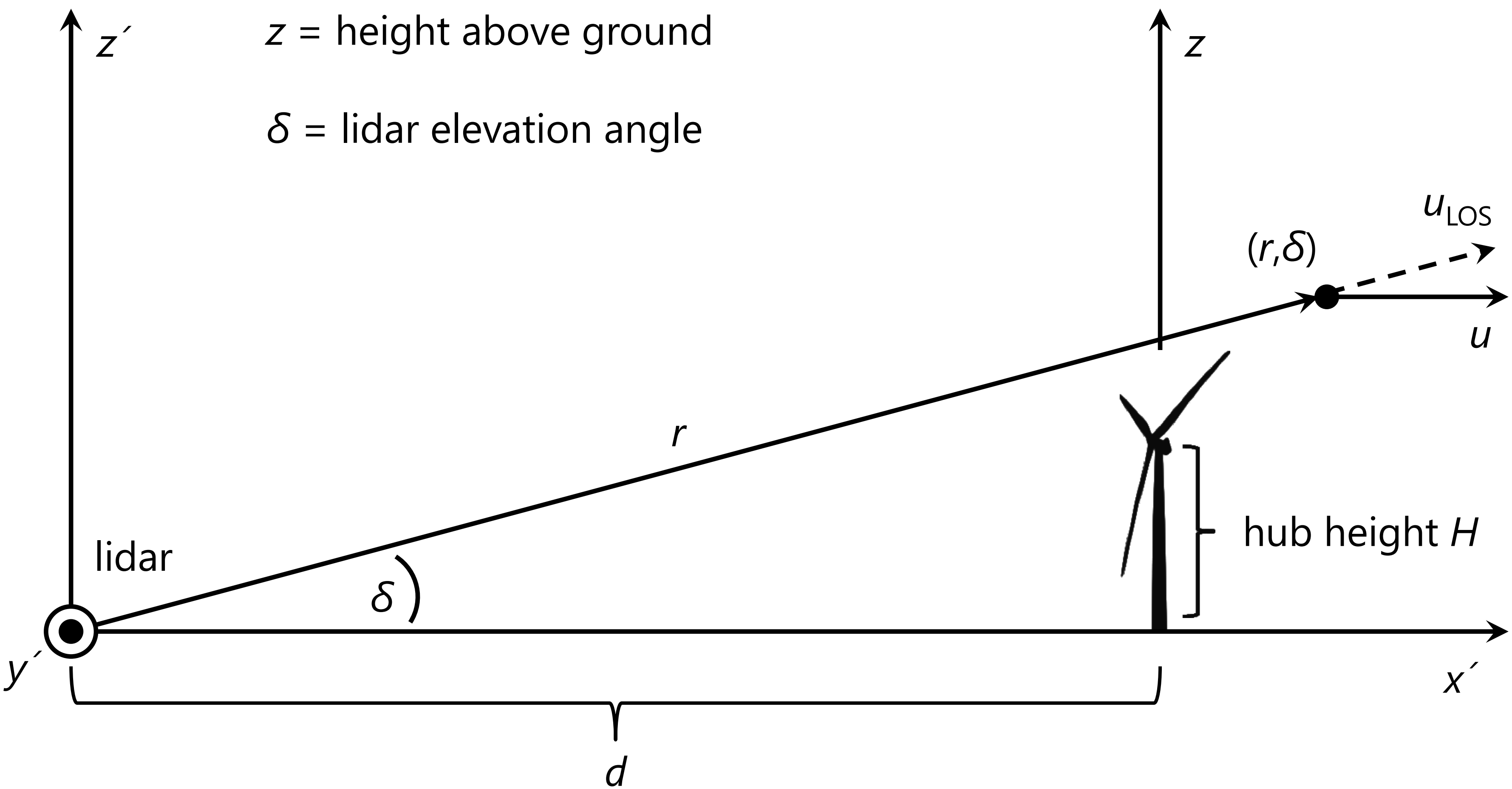

Aitken et al. (2014)
J. Atmos. Ocean. Tech., **31**, 765–787

Wake modeled as Gaussian subtracted from logarithmic wind speed profile

For each beam sweep, and at each range gate *r*, three models are fit to the lidar data to identify the wake, if any → Extra sum-of-squares F-test used to determine simplest model to fit data

$$u_{\mathrm{LOS}}(z,r) = \frac{u_*}{k}\ln\left[\frac{z}{z_0}\right]\cos\delta = \frac{u_*}{k}\ln\left[\frac{z}{z_0}\right]\sqrt{1-(z/r)^2}$$

ambient flow model

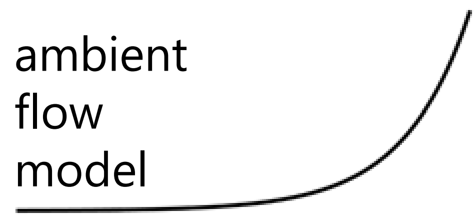

$$u_{\mathrm{LOS}}(z,r) = \left(\frac{u_*}{k}\ln\left[\frac{z}{z_0}\right] - a\exp\left[\frac{-(z-z_c)^2}{2s_h^2}\right]\right)\sqrt{1-(z/r)^2}$$

far wake model

$$u_{\mathrm{LOS}}(z,r) = \left(\frac{u_*}{k}\ln\left[\frac{z}{z_0}\right] - a\left\{\exp\left[\frac{-(z-z_l)^2}{2s_h^2}\right] + \exp\left[\frac{-(z-z_u)^2}{2s_h^2}\right]\right\}\right) \times\sqrt{1-(z/r)^2}$$

near wake model

Example fit to data from vertical scan

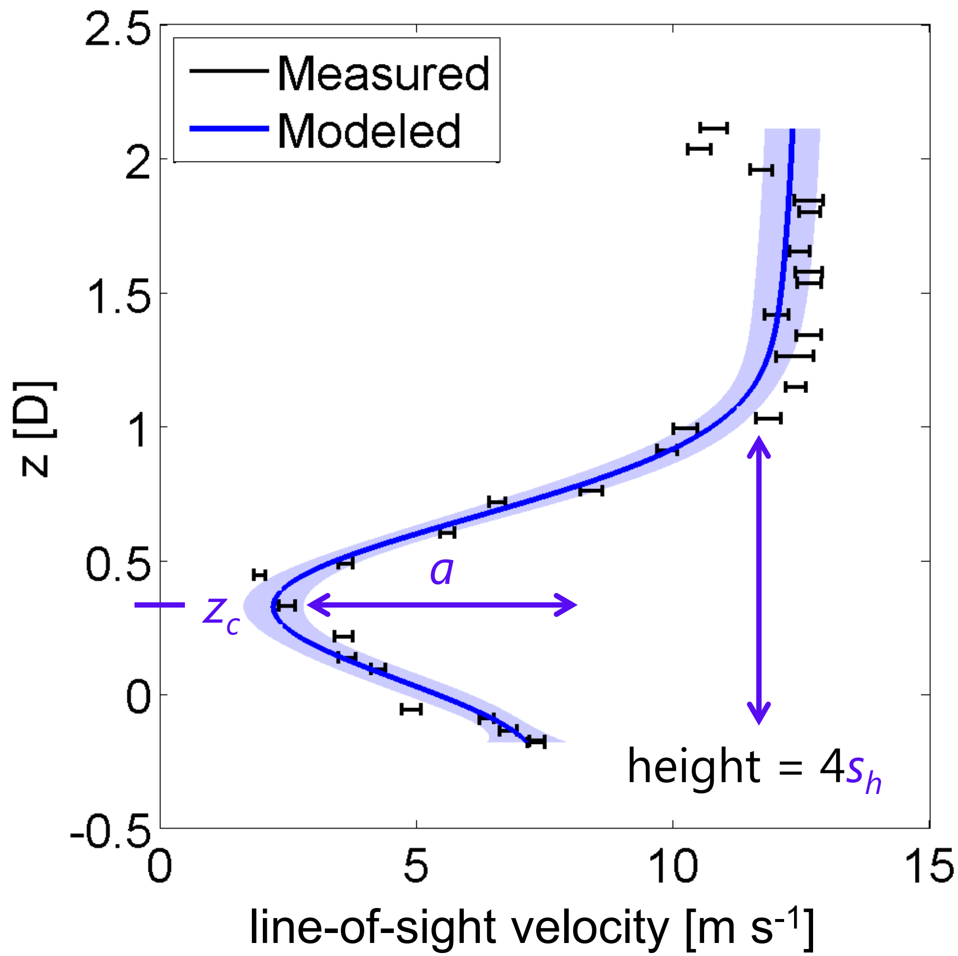

z_c: algorithm capable of tracking vertical location of wake center

wake height ≡ $4s_h$
(Hansen et al. 2012)

$$\text{velocity deficit} \equiv \frac{u_{ambient} - u_{wake}}{u_{ambient}} \times 100\%$$

$$u_{ambient} = \frac{u_*}{k} \ln\left[\frac{z_c}{z_0}\right]$$

$$u_{wake} = u_{ambient} - a$$

Aitken et al. (2014)
J. Atmos. Ocean. Tech., **31**, 765–787

Outline

- Lidar background
- Wind turbine wake characterization
  - theory and previous work
  - wake detection algorithm
  - **experiment**
  - simulation
- Summary

Lidar used to measure utility-scale turbine wakes in two experiments

	Experiment 1	Experiment 2
Location	National Wind Tech. Center	wind farm in western U.S.
Lidar type	ground-based | NOAA HRDL	nacelle-based | Galion G4000
Scan type	horizontal and vertical	horizontal
Data length	~100 hours	1 month
Reference	Aitken et al. (2014) *J. Atmos. Ocean. Tech.*, **31**, 765–787	Aitken/Lundquist (2014) *J. Atmos. Ocean. Tech.*, **31**, 1529–1539

Figs: NOAA and Windpower Engineering & Development

Nacelle-based lidar experiment conducted at a wind farm in the western U.S.

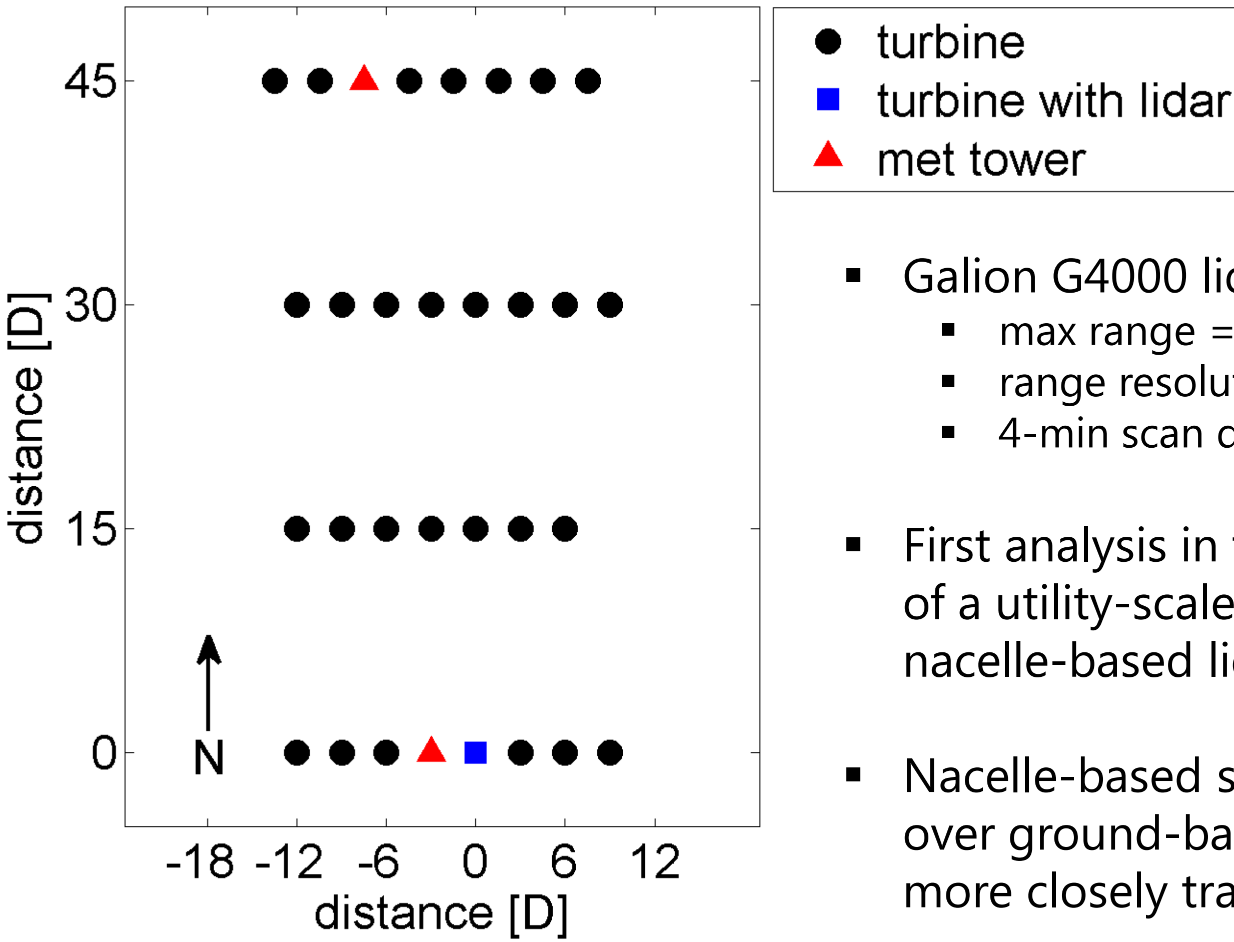

- Galion G4000 lidar
  - max range = 4 km
  - range resolution = 60 m
  - 4-min scan duration over 84° sector
- First analysis in the published literature of a utility-scale turbine wake using nacelle-based lidar
- Nacelle-based systems advantageous over ground-based ones b/c scans more closely transect wake centerline

Aitken and Lundquist (2014)
J. Atmos. Ocean. Tech., **31**, 1529–1539

Wake detection rate

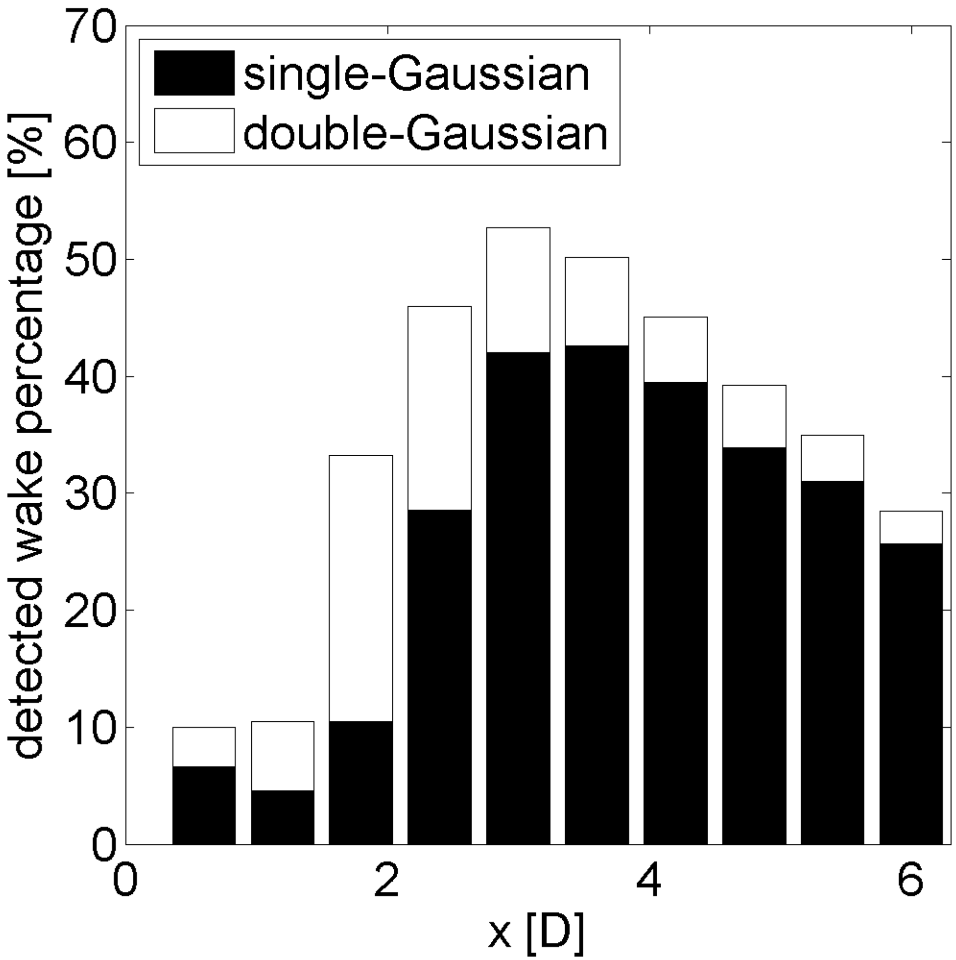

- Lidar field-of-view (84° sector) not wide enough to capture wake near the turbine
  - need larger scan sector in future experiments
- Near wake lasts until ~3D downwind
- Wakes detected w/ diminishing frequency after *x* = 3D
  - velocity deficit scales increasingly with ambient variability
  - velocity measurements are less precise at longer range gates
- Detection rate on par with España et al. (2011) *Wind Energy*, **14**, 923–937
  - particle image velocimetry in wind tunnel study

Aitken and Lundquist (2014)
J. Atmos. Ocean. Tech., **31**, 1529–1539

Velocity deficit decreases with downstream distance because of turbulent mixing

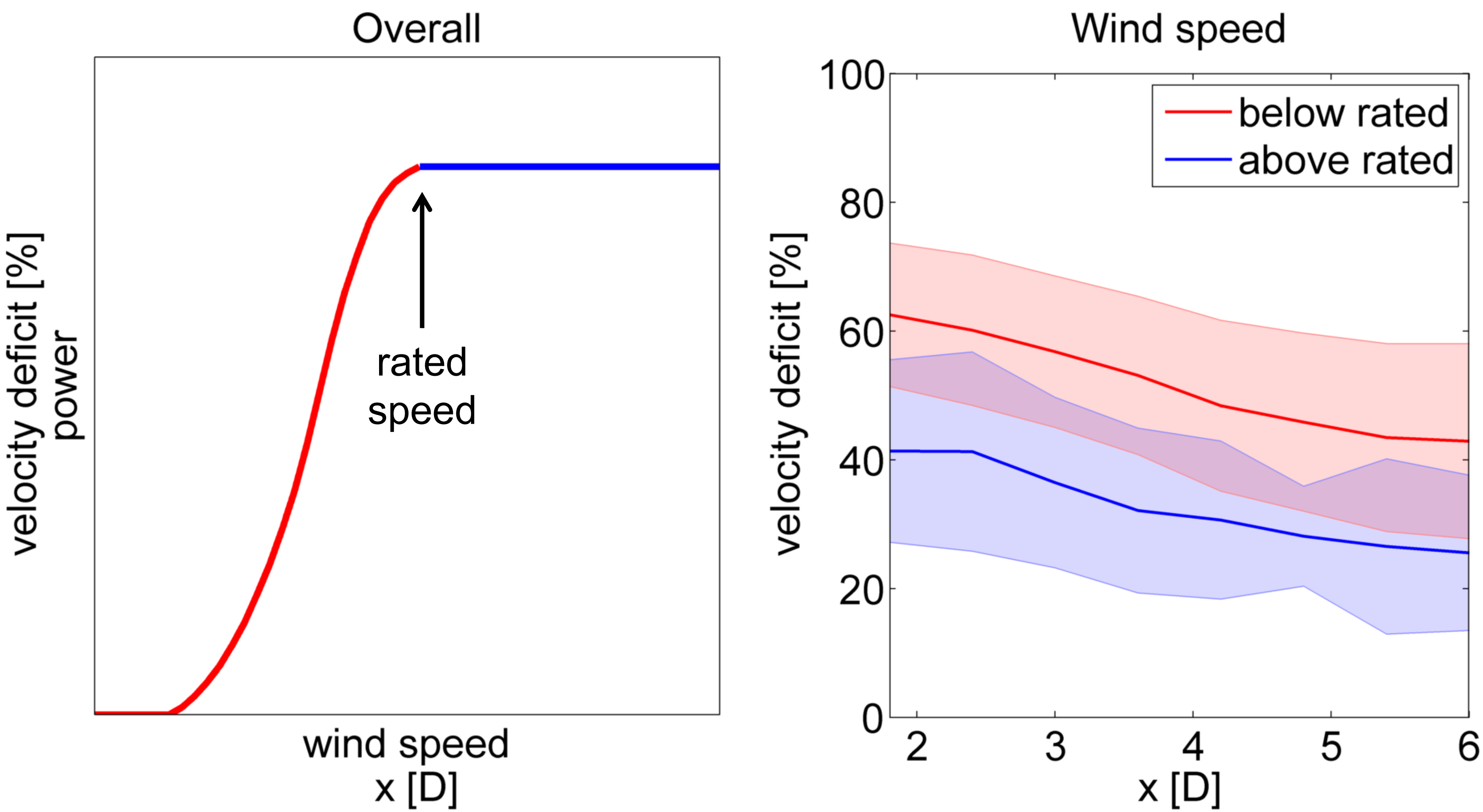

Aitken and Lundquist (2014)
J. Atmos. Ocean. Tech., **31**, 1529–1539

Wake boundary expands with downstream distance because of turbulent mixing

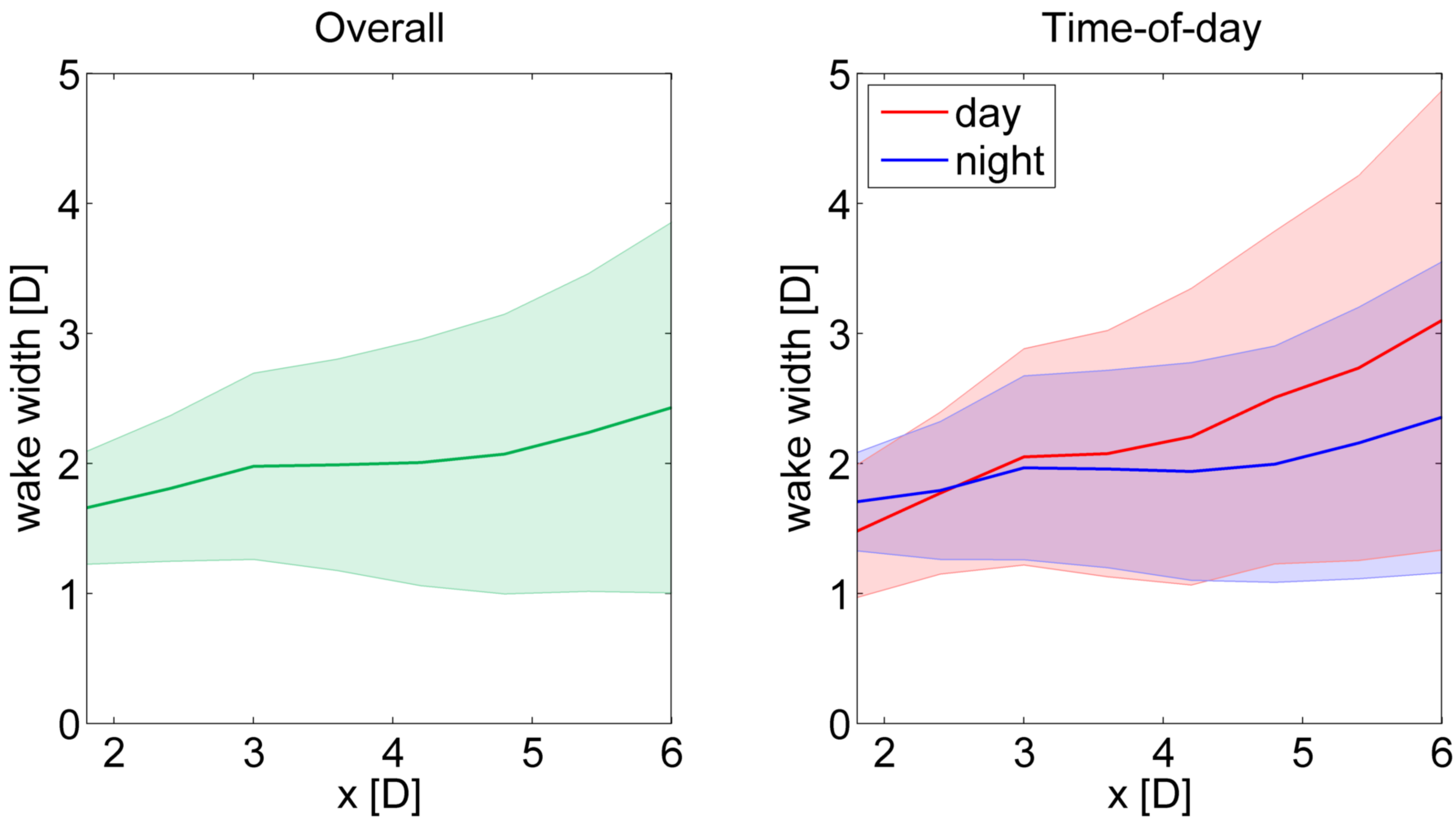

Aitken and Lundquist (2014)
J. Atmos. Ocean. Tech., **31**, 1529–1539

Outline

- Lidar background
- Wind turbine wake characterization
  - theory and previous work
  - wake detection algorithm
  - experiment
  - **simulation**
- Summary

Wind turbine performance depends on turbulence and atmospheric stability

- Rotating actuator disk model recently implemented in WRF-LES by Branko Kosović (NCAR) and Jeff Mirocha (LLNL)
  - comprehensive verification of this model requires simulating different turbines and atmospheric conditions

	Simulation 1	Simulation 2
Corresponding experiment	Experiment 1 (ground-based lidar @ NWTC)	Experiment 2 (nacelle-based lidar @ commercial wind farm)
Reference	Mirocha et al. (2014) *J. Renew. Sust. Energy*, **6**, 013104	Aitken et al. (2014) *J. Renew. Sust. Energy*, **6**, 033137
Stability	unstable	stable
Features	well-mixed surface heating convective cells thick boundary layer large characteristic eddies	wind shear surface cooling suppressed buoyancy shallow boundary layer small characteristic eddies

Rotating actuator disk model in WRF-LES implemented by Kosović and Mirocha

Blade Element Theory + Momentum Theory

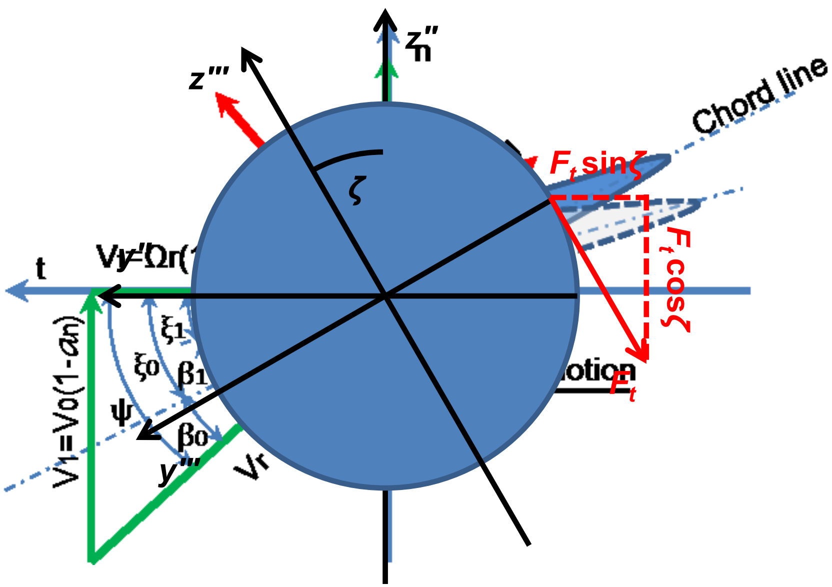

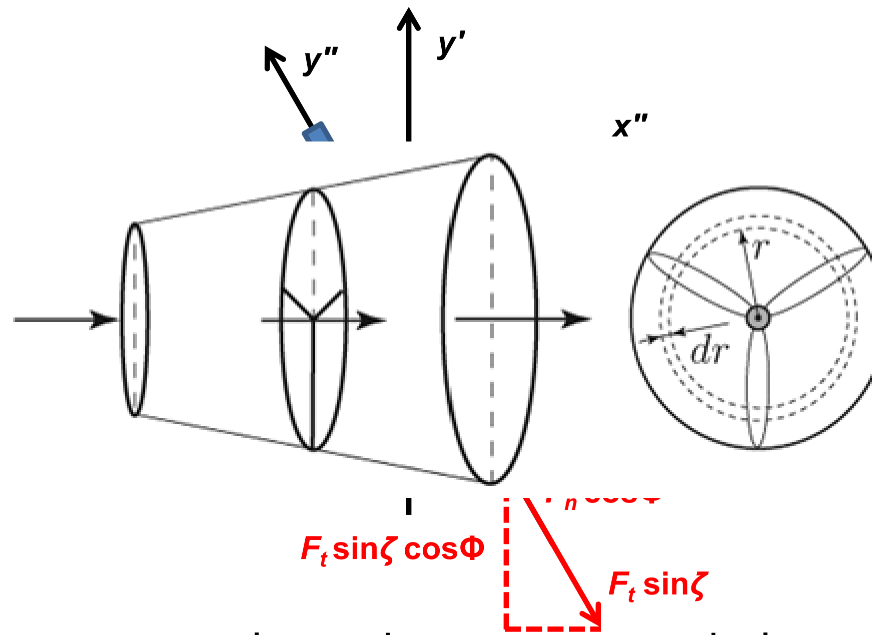

calculates the lift and drag forces generated by the airfoil at various sections along the blade

tangential force → rotation

analyzes the momentum balance on a rotating annular stream tube passing through the turbine

normal force → drag

Mirocha et al. (2014) *J. Renew. Sust. Energy*, **6**, 013104

Wang et al. (2013) *J. Sol. Energy Eng.*, **136**, 011018

Modifications to actuator disk model: rotor tilt (δ) and drag from tower/nacelle

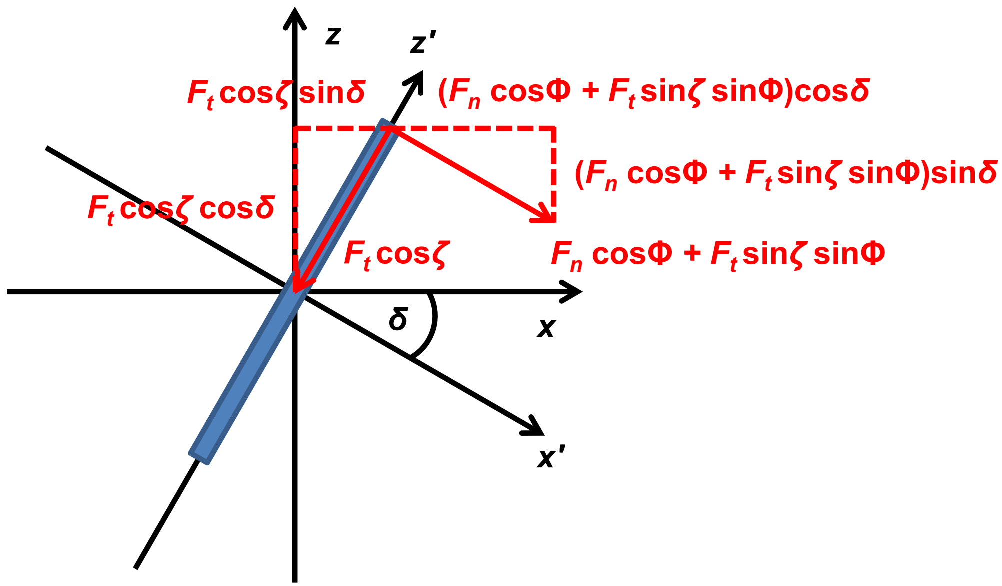

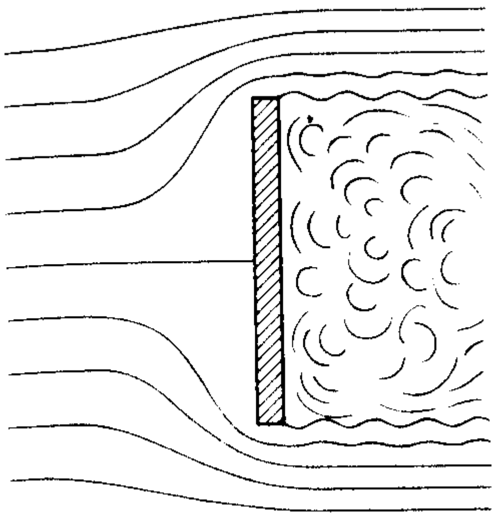

By Newton's third law, rotor tilt should cause the wake to be shifted upward

Aitken et al. (2014)
J. Renew. Sust. Energy, **6**, 033137

Case study

wind direction varied over a range of about 20 deg

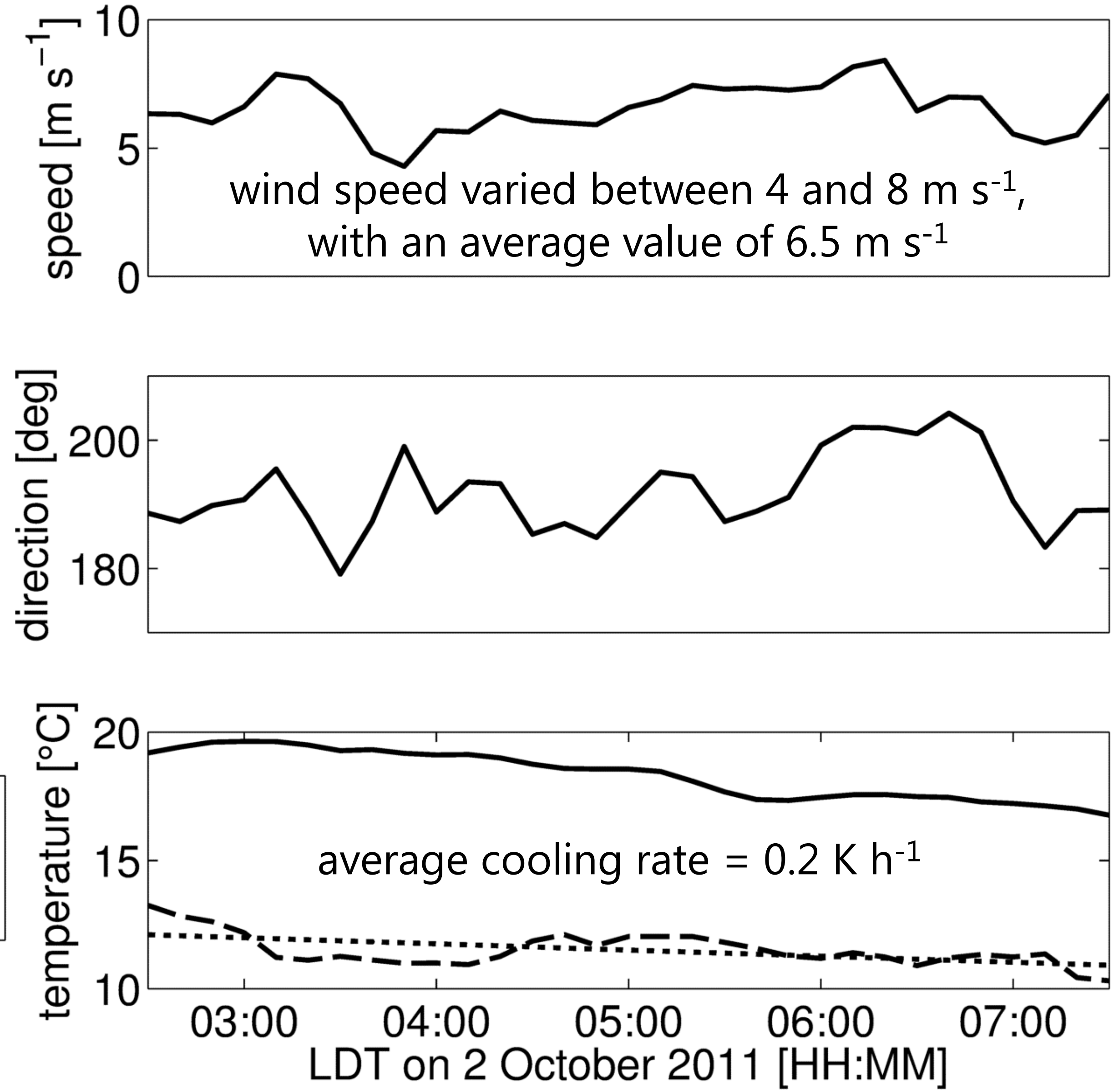

Aitken et al. (2014)
J. Renew. Sust. Energy, **6**, 033137

WRF simulation of wake dynamics

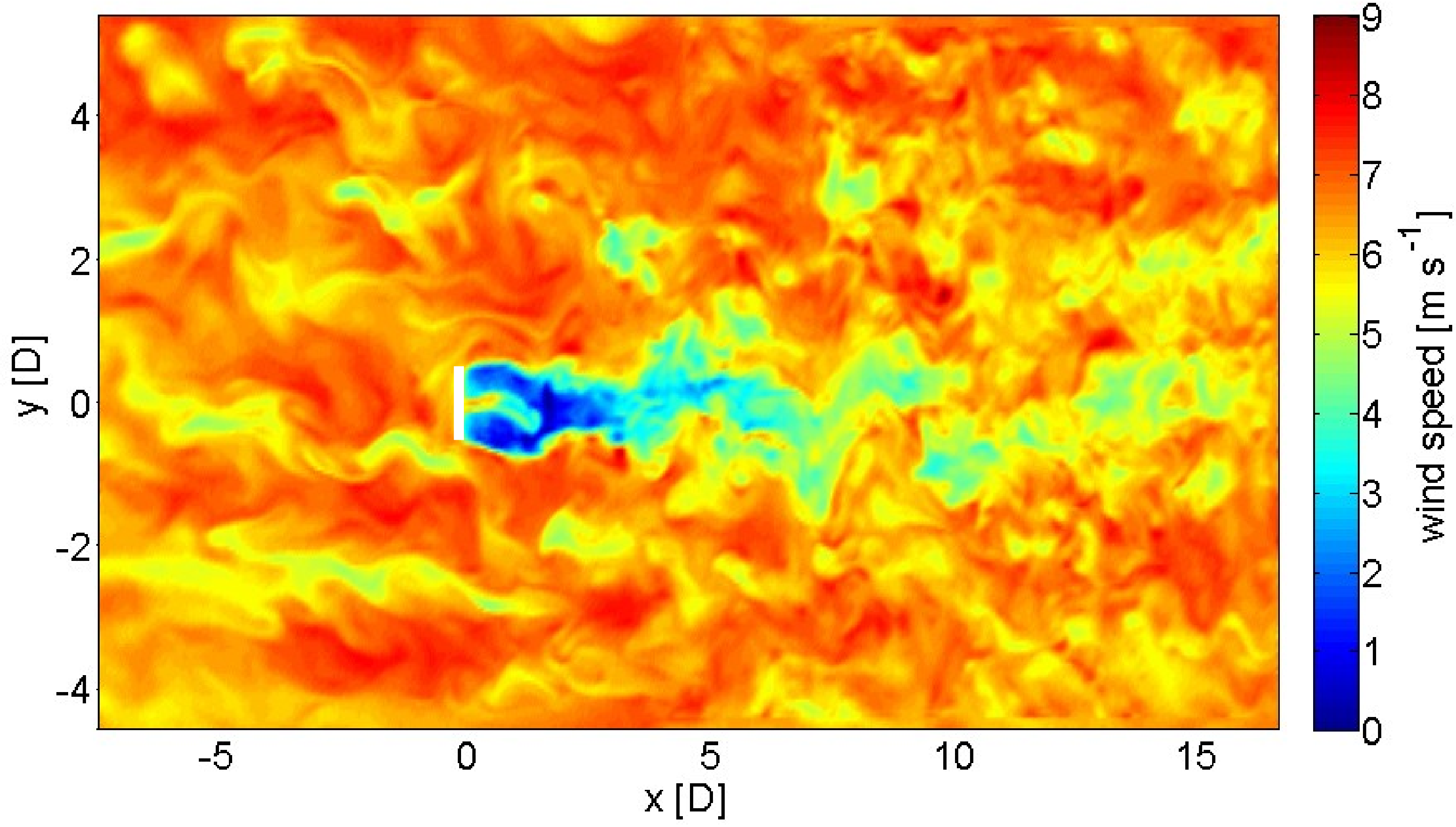

Simulated inflow conditions closely match met tower measurements

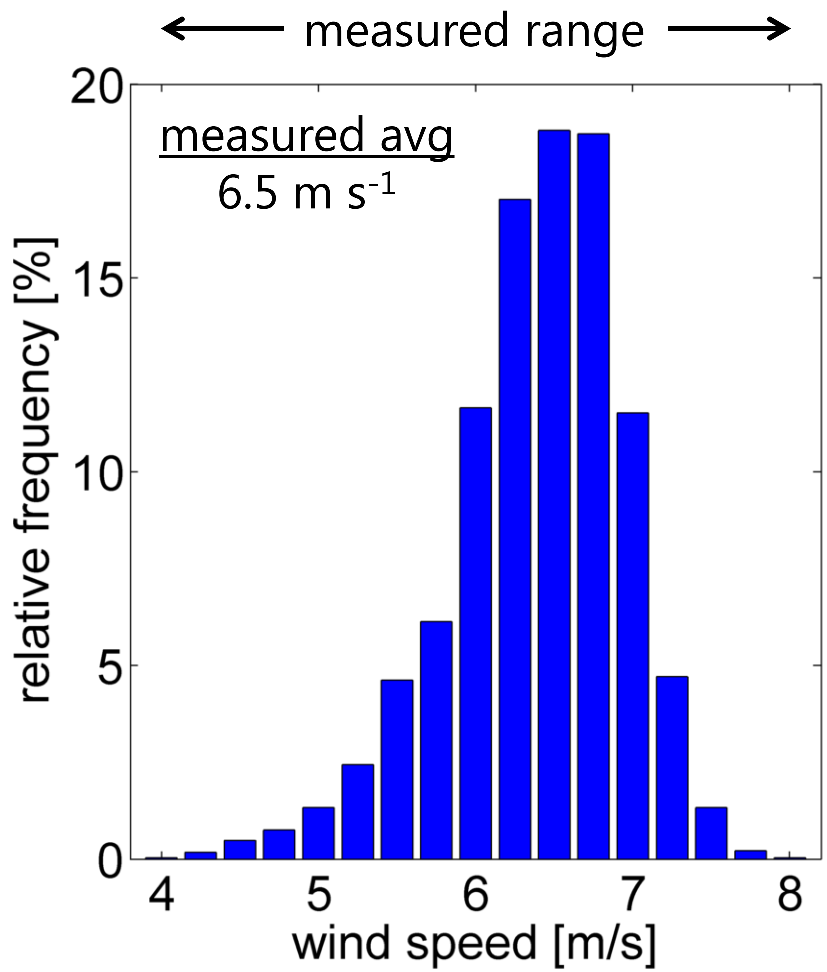

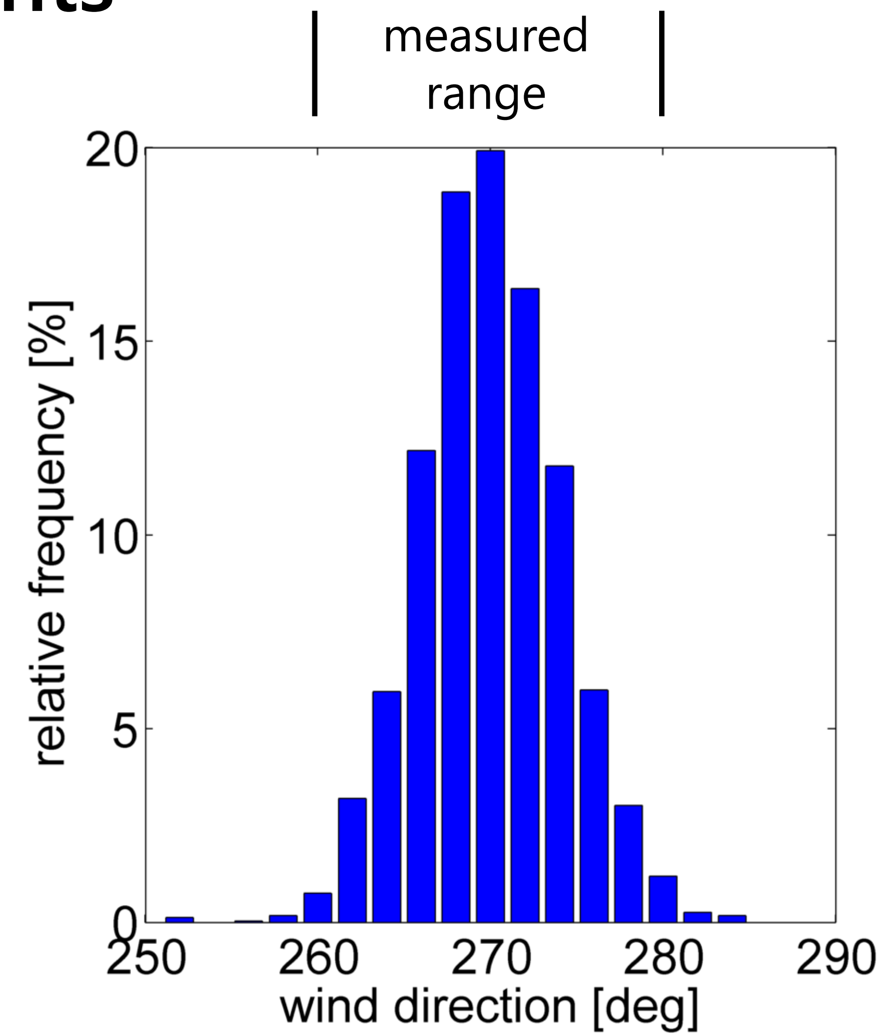

Aitken et al. (2014)
J. Renew. Sust. Energy, **6**, 033137

Simulation is capable of representing the transition from the near to far wake

Measured

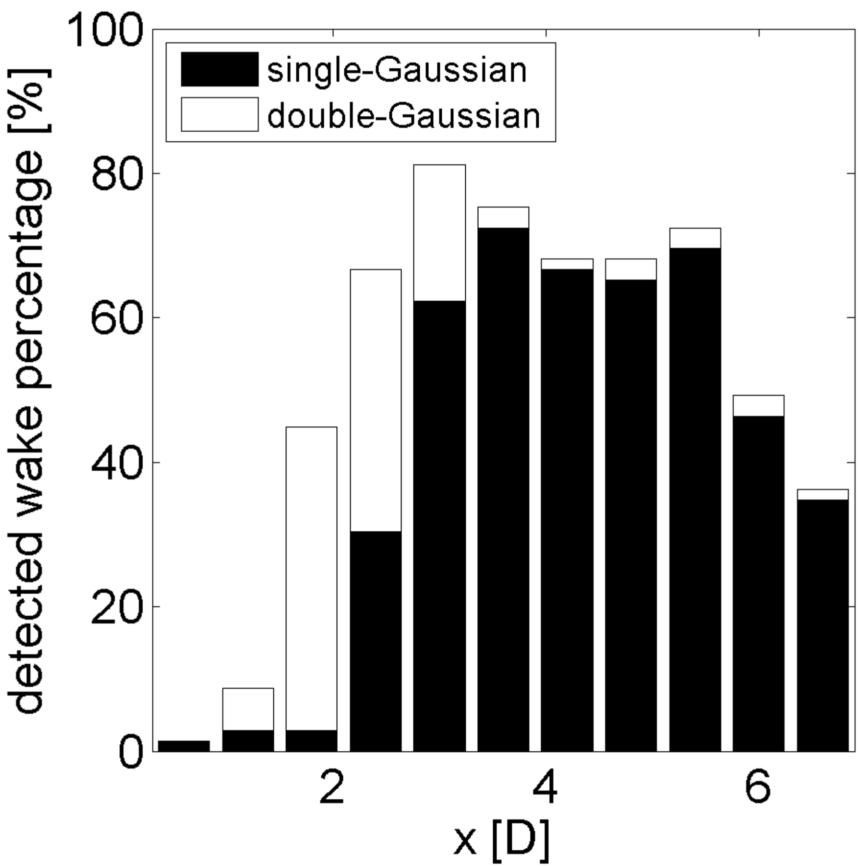

Simulated flow field transitions from a double-Gaussian to a single-Gaussian profile around *x* = 2–3D

Aitken et al. (2014)
J. Renew. Sust. Energy, **6**, 033137

Good agreement between measured and simulated results

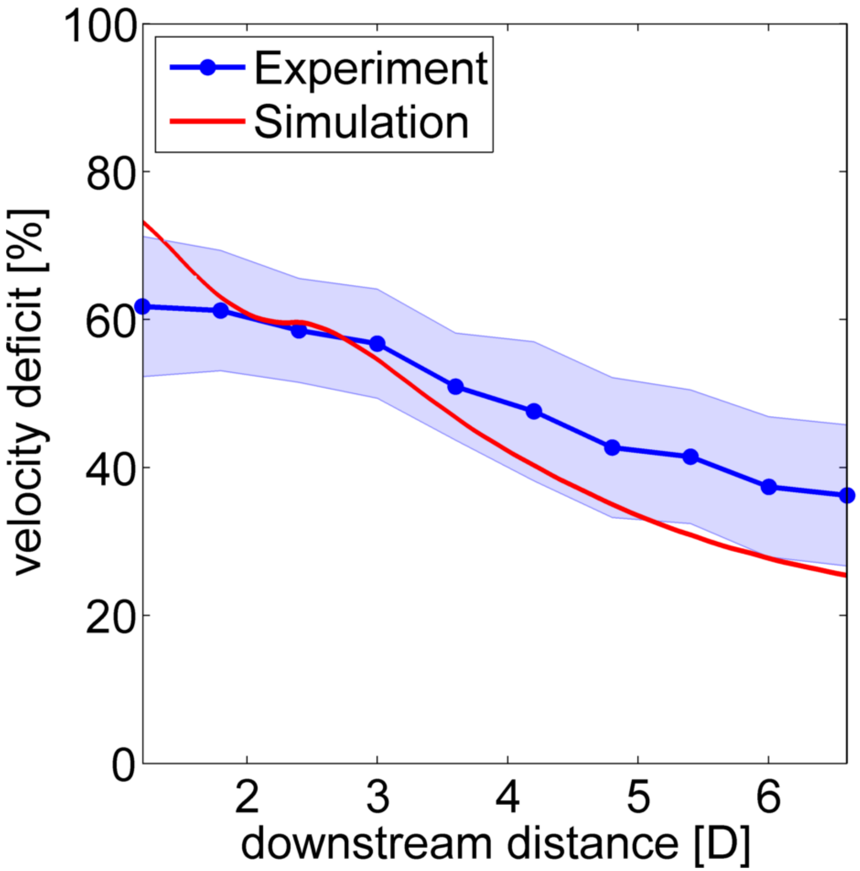

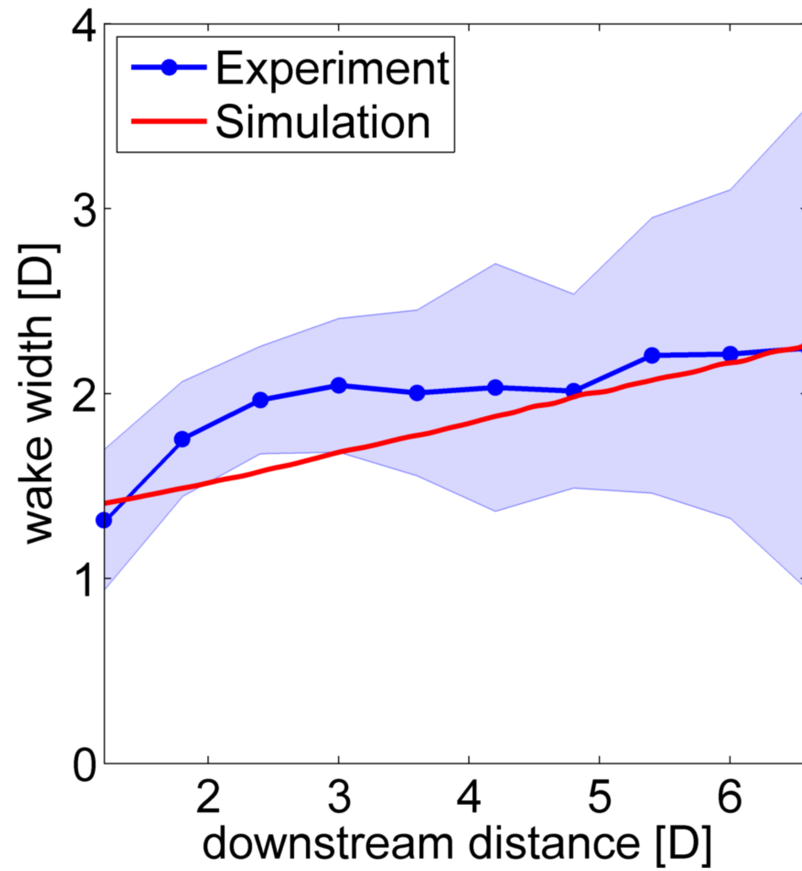

Aitken et al. (2014)
J. Renew. Sust. Energy, **6**, 033137

Vertical location of wake center is shifted upward because of rotor tilt

(analogous to results from Experiment 1)

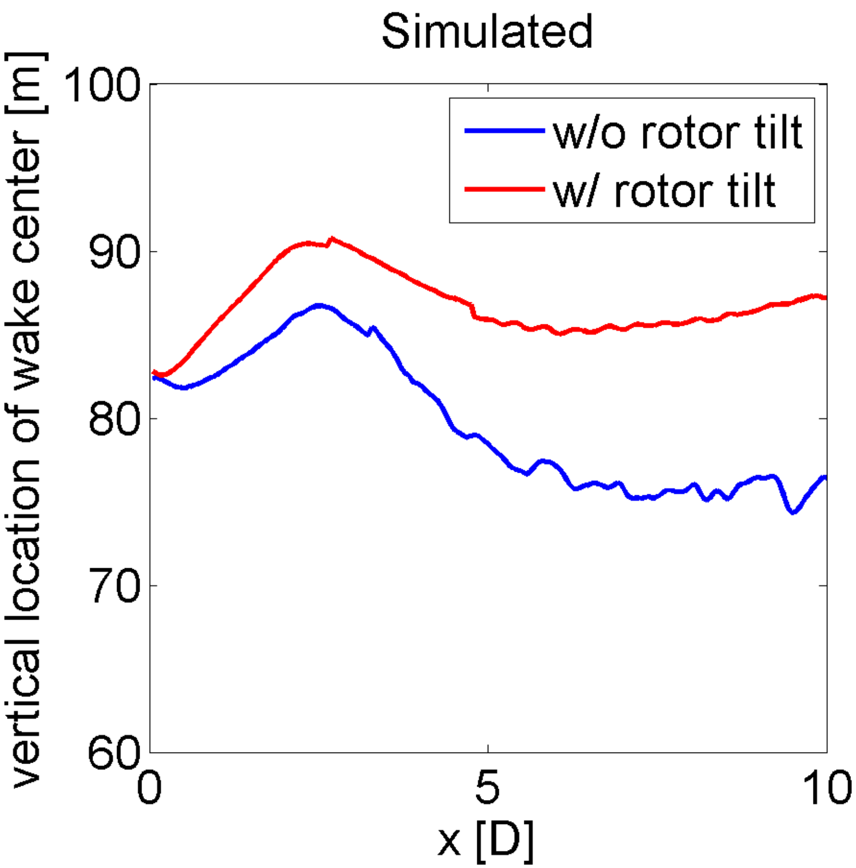

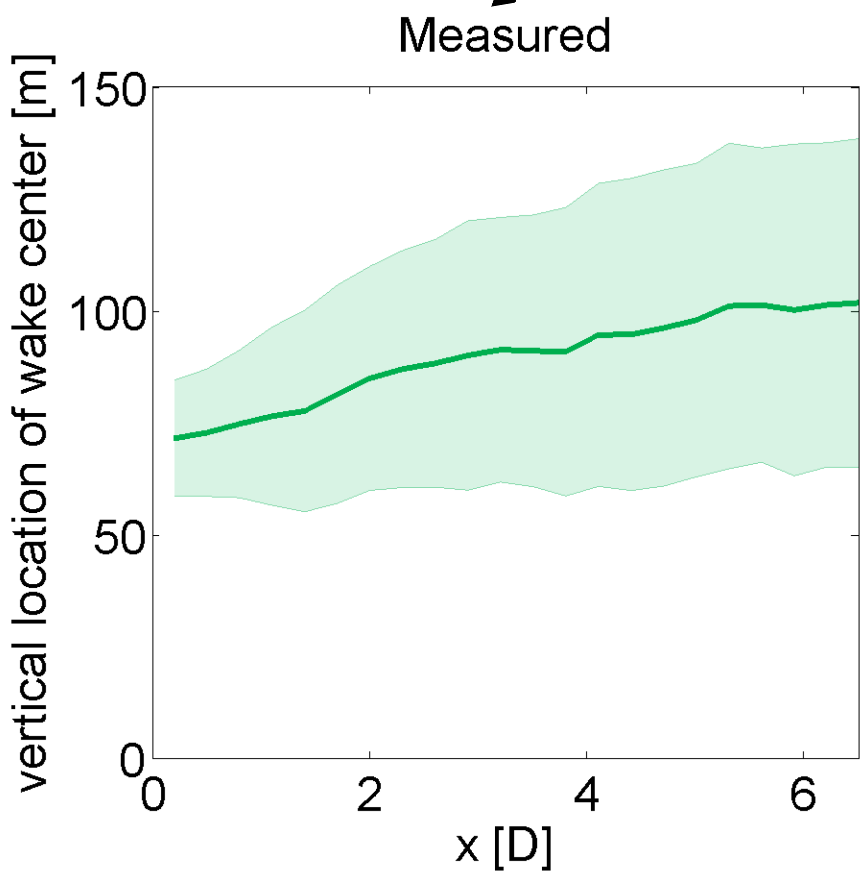

Aitken et al. (2014) *J. Renew. Sust. Energy*, **6**, 033137

Aitken et al. (2014) *J. Atmos. Ocean. Tech.*, **31**, 765–787

Outline

- Lidar background
- Wind turbine wake characterization
  - theory and previous work
  - wake detection algorithm
  - experiment
  - simulation
- **Summary**

Summary

- Developed statistical model for wind turbine wake characterization
  - generally applicable to experiment and simulation
  - allows for categorization of results by atmospheric conditions
- Conducted first analysis of utility-scale turbine wake using nacelle-based lidar
- Simulated stable conditions
- Added rotor tilt and tower/nacelle drag to actuator disk model in WRF-LES
  - demonstrated upward shift in wake centerline
- Good agreement between measured and simulated results

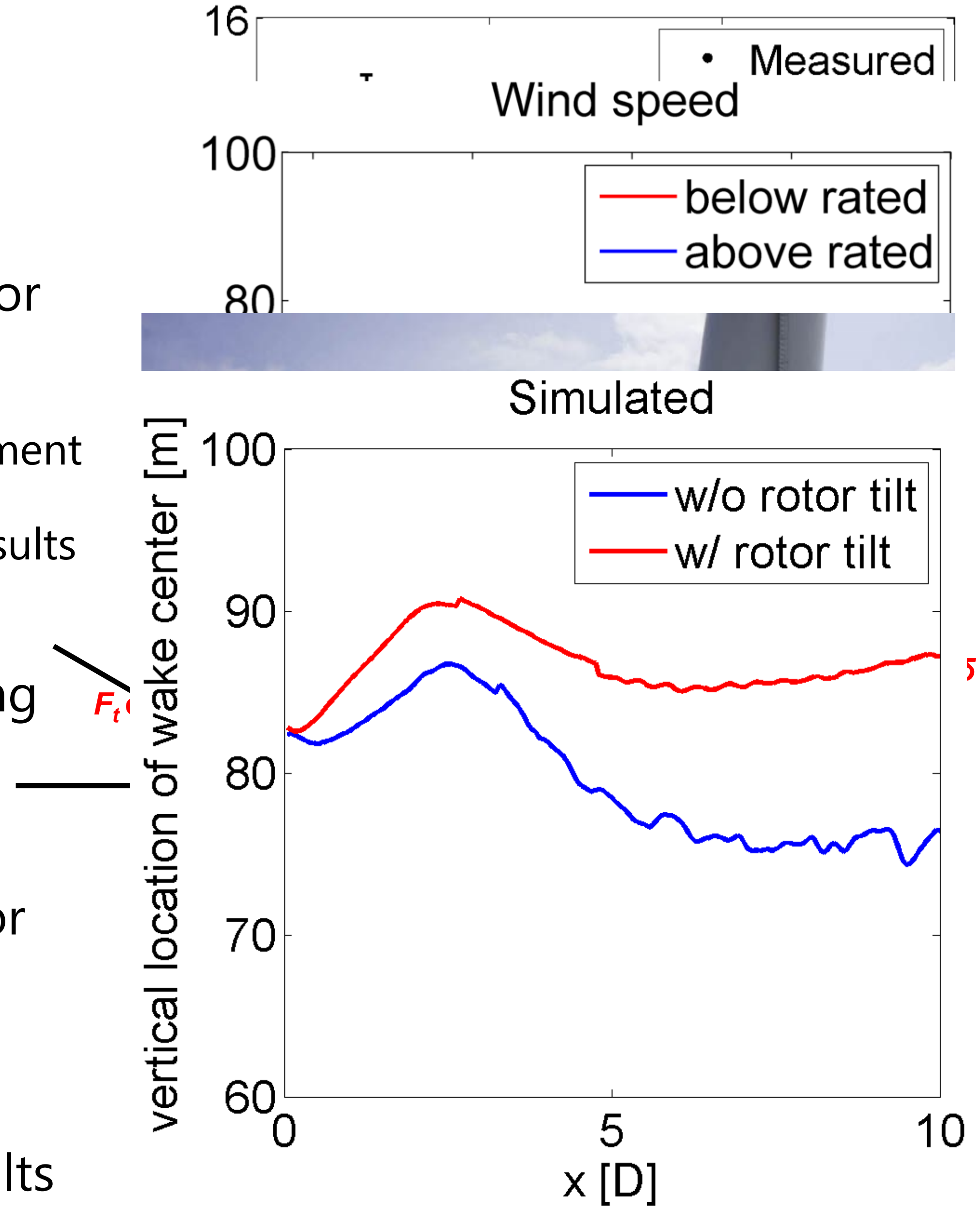

Thank you

Fig: John De Bord Photography